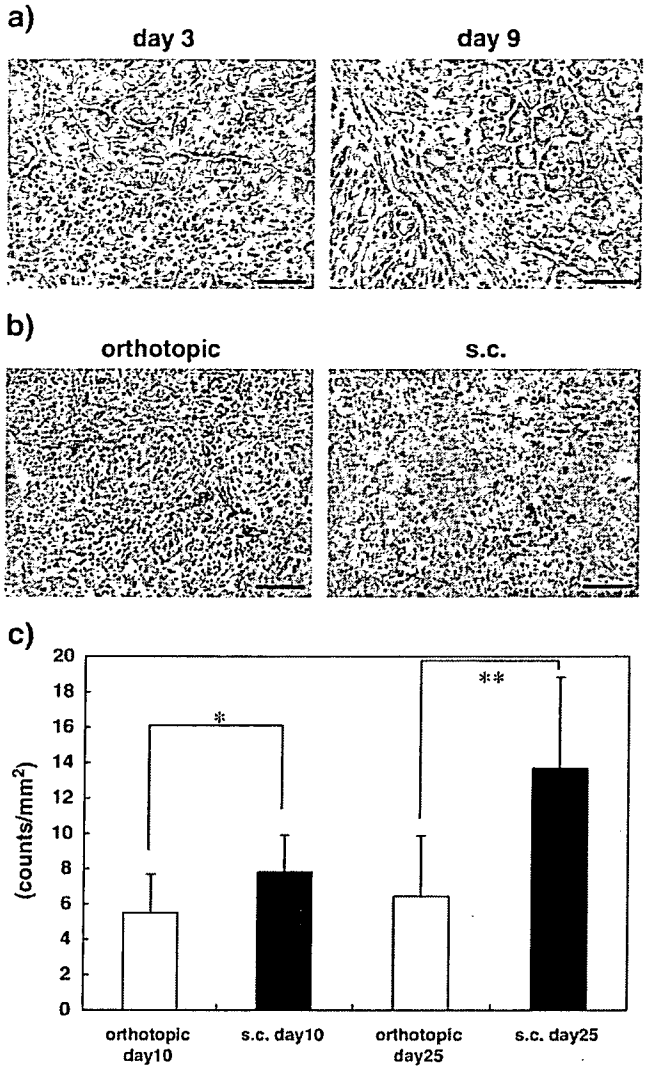

Fig. 1. Characteristics of orthotopic pancreatic tumor model. SUIT-2 cells (5×10^6 cells) were implanted into the pancreas of BALB/c nude mice. At day 3 and 9 after the tumor implantation, mice were sacrificed and tumor sections were prepared as described in Materials and methods. Then they were stained with hematoxylin and eosin (a). On the day 10 and 25, tumor sections were also prepared for evaluating vasuclarization. The sections were immunostained with biotinylated anti-mouse CD31 monoclonal antibody, and visualized with DAB as colorimetric substarate (b) or streptavidin-Alexa fluor® 488 conjugated-second antibody. CD31 positive area was observed fluorescently by a laser scanning microscopy and was quantified by ImageJ software (c). Significant differences are shown with asterisks: *, $p<0.05$ and **, $p<0.01$. Scale bar represents 100 μm.

previously [14]. In brief, lipids were dissolved in chloroform or chloroform/methanol, dried under reduced pressure, and stored *in vacuo* for at least 1 h. Then, the liposomes were formed by hydration of the thin lipid film with 0.3 M glucose, and frozen and thawed for 3 cycles using liquid nitrogen. Then liposomes were sized by thrice extrusion through a polycarbonate membrane filter with 100-nm pores. For a biodistribution study, a trace amount of [^{3}H]-cholesterylhexadecylether (Amersham Pharmacia, Buckinghamshire, UK) was added to the initial chloroform/methanol solution as described above. To observe the intratumoral distribution of liposomes, they were fluorescently labeled with 1,1′-dioctadecyl-3, 3, 3′, 3′-tetramethylindocarbocyanine perchlorate (DiI C_{18}; Molecular Probes Inc., Eugene, OR, USA), which was added to them at the quantity equivalent to 1 mol% of DSPC. For therapeutic experiment, ADM-encapsulated liposome was prepared by a modification of the remote-loading method as described previously [14]. The concentration of ADM was determined at 484 nm absorbance.

2.7. Biodistribution of liposome

Biodistribution study was performed at day 10 after SUIT-2 tumor implantation. Orthotopic pancreatic tumor model mice were injected with radiolabeled liposomes containing [^{3}H] cholesterylhexadecylether *via* a tail vein. Three or twenty-four hours after injection, the mice were sacrificed under diethyl ether anesthesia for the collection of the blood. Then the blood was centrifuged (600 ×*g* for 5 min) to obtain the plasma. After the mice had been bled from the carotid artery, the heart, lung, liver, spleen, kidney and tumor were removed, washed with saline and weighed. The radioactivity in each organ as well as plasma was determined with a liquid scintillation counter (Aloka LSC-3100). Distribution data are presented as % dose per 100-mg wet tissue, where the total amount in plasma was calculated based on the average mice body weight, which was 25.5 g and average plasma volume, which was assumed to be 4.27% of body weight based on the data of total blood volume. The animals were cared for according to the animal facility guidelines of the University of Shizuoka.

2.8. Intratumoral distribution of liposome

DiI C_{18}-labeled liposomes were administered *via* a tail vein of mice with orthotopic pancreatic tumor on the day 3, 9 and 18

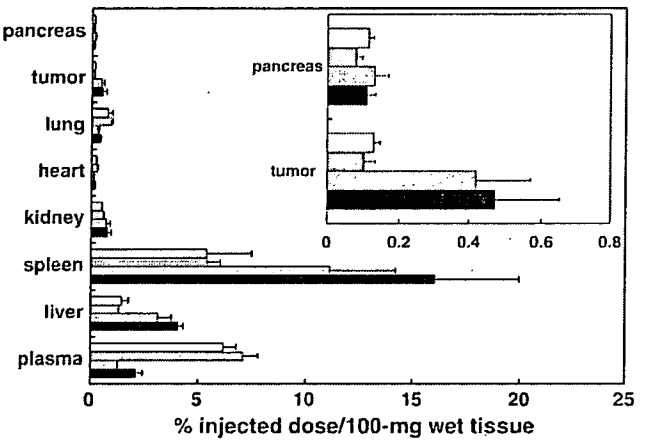

Fig. 2. Biodistribution of ^{3}H-labeled liposomes in various organs. Orthotopic pancreatic tumor model mice were injected with ^{3}H-labeled-PEG-modified liposome or APRPG-PEG-modified liposome *via* a tail vein at day 10 after tumor implantation. Three and twenty-four hours after injection, mice were dissected and the radioactivity in each organ was determined ($n=3$). Data are presented as percent of the injected dose per 100 mg tissue and S.D. Inset indicates the liposomal accumulation in the tumor and in pancreas represented as the percent-injected dose per 100 mg wet tissue. Data represents 3 h PEG-Lip (open bar), 3 h APRPG-PEG-Lip (dark gray bar), 24 h PEG-Lip (light gray bar) and 24 h APRPG-PEG-Lip (closed bar), respectively.

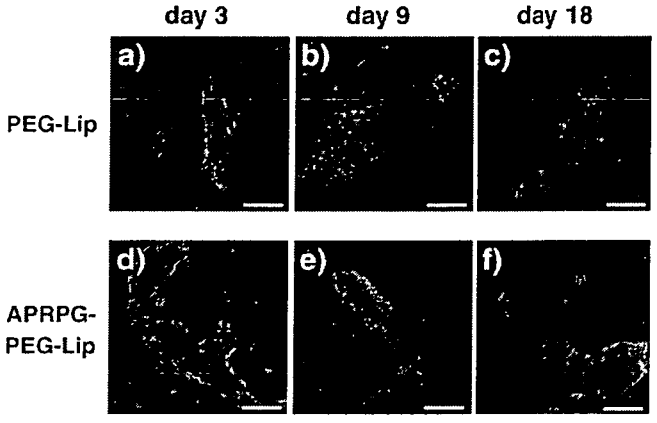

Fig. 3. Intratumoral distribution of $DiIC_{18}$-labeled liposomes. Orthotopic pancreatic tumor model mice were injected with PEG-Lip (a–c) or APRPG-PEG-Lip (d–f) labeled with $DiIC_{18}$ *via* a tail vein at day 3 (a, d), day 9 (b, e), and day 18 (c, f) after tumor implantation. At 2 h after injection of fluorescence-labeled liposomes, frozen-sections of each tumor were prepared. Green portions indicate CD31-positive regions, red portions liposomal distribution, and yellow portions show the localization of liposomes at the site of vascular endothelial cells. Scale bar represents 50 μm.

after tumor implantation. Two hours after injection of liposomes, mice were sacrificed under diethyl ether anesthesia and the tumor was dissected. Preparation of tumor sections and CD31 staining were performed as described in the Section 2.5. These tumor sections were fluorescently observed by using microscopic LSM system (Carl Zeiss, Co., Ltd.): Endothelial cells were identified as green fluorescence and liposomes were detected as red.

2.9. Therapeutic experiment

Orthotopic pancreatic tumor model was prepared by the injection of SUIT-2 cells (5×10^6 cells/mouse). Liposomes encapsulating ADM or 0.3 M glucose solution were administered intravenously into SUIT-2-bearing mice at day 3, 6, 9 and 12 after the tumor cell implantation. The injected dose of liposomal ADM in each administration was 10 mg/kg as ADM. The weight of tumor was examined at day 15. For histochemical analysis, the sections of tumor were prepared, and then immunostaining with anti-CD31 antibody and hematoxylin-eosin staining were performed as described above.

2.10. Statistical analysis

Student's *t*-test was used for statistical analysis, and $p<0.05$ were considered to be statistically significant.

3. Results

3.1. Preparation of orthotopic pancreatic tumor model

At first, we examined the characteristics of orthotopic pancreatic tumor model by using SUIT-2 human pancreatic tumor cell line. Histopathological examination indicated that tumor cells invaded into neighboring pancreatic tissue at 3 and 9 days after tumor implantation (Fig. 1a). Then we investigated whether the model showed hypovascular characteristics or not. For this purpose, vascular density of the model was compared with that of s.c. implanted SUIT-2 tumor model. The result of immunostaining with anti-CD31 antibody showed that MVD of orthotopic pancreatic tumor model was lower than that of s.c. implanted model (Fig. 1b): The significant differences were observed in CD31 positive area of day 10-orthotopic model mice from that of day 10-s.c. model mice ($p<0.05$), day 25-orthotopic model mice from day 25-s.c. model mice ($p<0.01$). These data indicated that orthotopic implantation of SUIT-2 cells developed pancreatic tumor with hypovascular characteristics. The immunostaining study also confirmed the hypovascular characteristics of the orthotopic pancreatic tumor model (Fig. 1c).

3.2. Biodistribution of liposomes

Before therapeutic experiment, we investigated the biodistribution of the liposome in the orthotopic pancreatic tumor-bearing mice, since the accumulation of drug carrier is prerequisite for the therapeutic effect of entrapped drugs in the carrier at the target site. Ten days after SUIT-2 tumor implantation, ^{3}H-labeled PEG-Lip or APRPG-PEG-Lip was injected *via* a tail vein. Three and twenty-four hours after injection of liposomes, mice were sacrificed and tumor and other organs were dissected for measuring the radioactivity in these tissues. Both PEG-Lip and APRPG-PEG-Lip accumulated in tumor time-dependently, although there was no significant difference between those two kinds of liposomes (Fig. 2). Therefore, even though in the hypovascular tumor, enhanced permeability and retention (EPR) effect of liposomes is achieved to some extent.

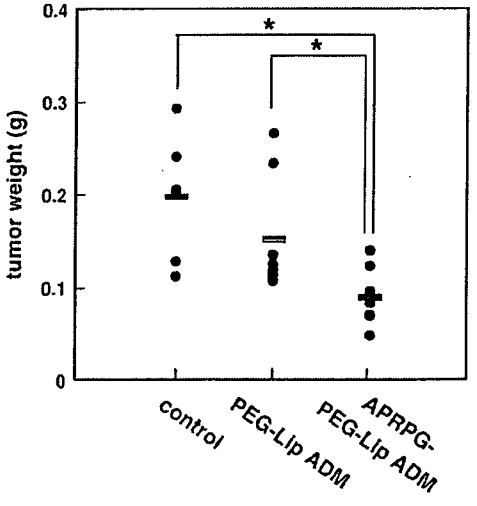

Fig. 4. Therapeutic effect of APRPG-PEG-modified liposome encapsulating ADM on orthotopic pancreatic tumor model mice. Orthotopic pancreatic tumor model mice were injected *i.v.* with 0.3 M Glucose (control), PEG-LipADM or APRPG-PEG-LipADM for 4 times at day 3, 6, 9 and 12 after tumor implantation ($n=6$–8). Injected dose of liposomal ADM were adjusted to 10 mg/kg as ADM concentration in each time. The weight of the tumors was measured at day 15. Significant differences are shown with asterisks: *, $p<0.05$.

3.3. Intratumoral distribution of liposomes

Next, we determined intratumoral distribution of the liposomes in the present hypovascular tumor model. Three, nine and 18 days after tumor implantation, DiI C_{18}-labeled liposomes were injected *via* a tail vein of SUIT-2 orthotopically implanted mice. Two hours after injection, frozen section of tumor was prepared. After fluoroimmunostaing with CD31 antibody, the intratumoral distribution of liposomes was observed with confocal laser scan microscopy. As shown in Fig. 3a–c, red fluorescence indicating PEG-Lip localization was observed in vascular like structure of CD31-staining (green fluorescence). On the contrary, fluorescence of APRPG-PEG-Lip was observed not only in the vessel like structure but also with CD31-staining, suggesting that APRPG-PEG-Lip was associated with angiogenic endothelial cells.

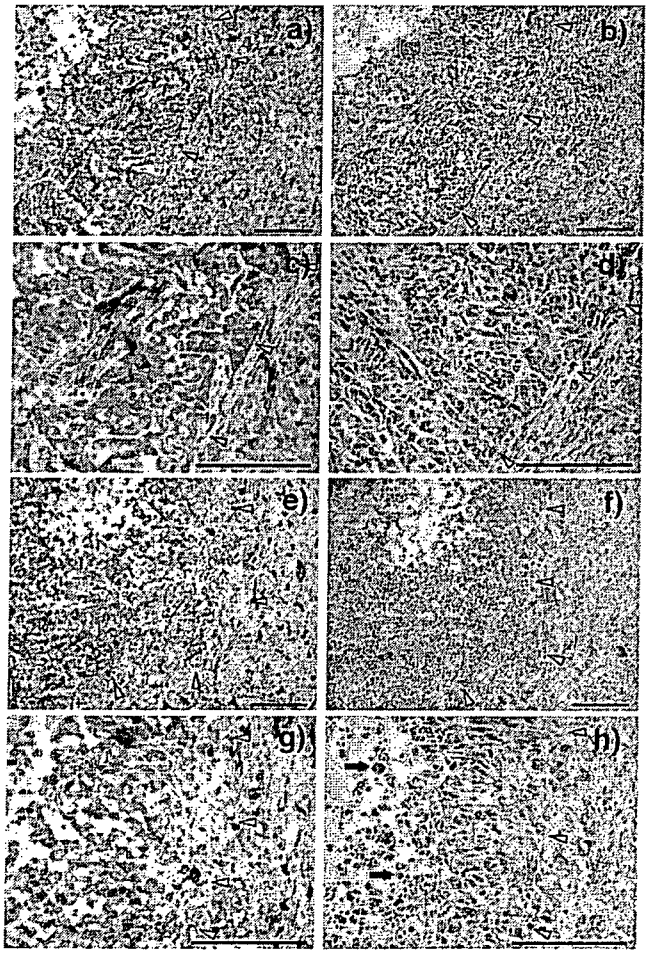

Fig. 5. Immunohistochemical analysis of dissected tumor after the treatment tumor model mice with APRPG-PEG-modified liposome encapsulating ADM. Orthotopic pancreatic tumor model mice were treated as described in the legend of Fig. 4. Tumor sections were prepared from the mice treated with PEG-LipADM (a–d) or with APRPG-PEG-LipADM (e–h). The sections were immunostained with biotinylated anti-mouse CD31 monoclonal antibody and visualized with DAB, and then co-stained with hematoxylin (a, c, e, g), or stained with hematoxylin-eosin (b, d, f, h). Arrowheads indicate the boundary of normal and tumor tissues, and arrows in (h) indicate macrophages. Scale bar represents 100 μm.

3.4. Therapeutic experiment by use of ADM-loaded liposomes

To examine the therapeutic effect of neovessel-targeted liposomal ADM on the orthotopic pancreatic tumor model mice, ADM-encapsulated APRPG-PEG-modified liposome (APRPG-PEG-LipADM) or ADM-encapsulated PEG-modified liposome (PEG-LipADM) were injected *via* a tail vein of the mice at 3, 6, 9 and 12 days after the tumor implantation. At day 15, tumor was removed and weighed to evaluate the effect of the treatment. As shown in Fig. 4, the significant differences in tumor weight of APRPG-PEG-LipADM-treated group from control ($p<0.05$) and PEG-LipADM-treated group ($p<0.05$) were observed. We also examined the body weight change of these mice after tumor implantation as an indicator of side effects, and observed that no significant difference between the three groups tested (data not shown).

Finally the sections of dissected tumor tissues were examined by immunostaining of CD31 and hematoxylin-eosin staining. As shown in Fig. 5, CD31-positive cells were observed in the tumor to some extent after treatment with PEG-LipADM. On the contrary, vessel-like structures were disappeared in the tumor after treatment with APRPG-PEG-LipADM, suggesting that APRPG-PEG-LipADM degenerated neovessels inside the tumor. Furthermore, the invasion of macrophages into the tumor was observed in the latter case.

4. Discussion

General anti-angiogenic therapy is based on the inhibition of the angiogenic cascade such as receptor binding of VEGF, signal transduction of VEGF, migration of proliferating endothelial cells, and tube formation. However, it is uncertain that the inhibition of angiogenic cascade is able to lead tumor regression. ANET is different from the traditional anti-angiogenic therapy, since this therapy eradicates proliferating endothelial cells and is expected to eradicate tumor cells through complete cutoff the blood supply to tumor tissues resulting in regression of the tumors. Moreover, ANET would not be expected to acquire drug-resistance, and would inhibit hematogenous metastases.

In here, we showed the therapeutic efficacies of ANET in orthotopic pancreatic tumor model by using tumor neovasculature-targeted liposome encapsulating an anti-cancer drug, ADM. Since pancreatic cancer is known as hypovascular cancer, injury of the small number of vascular cells may affect on large extent of cells that depend on supply of oxygen and nutrients to the vessel. Many experiments have been done to treat pancreatic tumor by anti-angiogenic therapy. These results, however, suggest that the effect of anti-angiogenic therapy alone is thought to be inadequate, concomitant treatments with anti-cancer drug or radiation have been tried [16,17]. On the other hand, ANET injures the proliferative angiogenic endothelial cells directly, and is expected to cause complete regression of tumor cells.

At first, we confirmed the model used here had characteristics of hypovascular tumor. As shown in Fig. 1, the CD31 positive area of orthotopic tumor model is significantly smaller

than that of s.c. implanted tumor. The efficiency of ANET in previous study was the case of s.c. implantation model [14]. The present study is for the first time to investigate whether ANET works in hypovascular tumor model. Biodistribution study by using ^{3}H-labeled PEG-Lip and APRPG-PEG-Lip showed no differences in the accumulation of liposome in the tumor. In general, PEG-modification prevents liposomes from opsonization and reticuloendothelial system (RES)-trapping [18]. This enables liposomes to circulate a long time in bloodstream and to accumulate in the interstitial spaces of tumor tissue through leaking out of angiogenic vessels: This behavior is due to so-called EPR effect [19,20], and such accumulation is called as passive targeting. APRPG peptide-modification adds an ability to actively interact with the angiogenic vessels, although the total accumulation of PEG-Lip and APRPG-PEG-Lip in the tumor was not significantly different. This result is consistent with our previous study using s.c. implanted tumor. We previously observed that the accumulation of PEG-Lip and APRPG-PEG-Lip was quite similar in s.c. implanted tumor model [14], but the intratumoral distribution was much different: PEG-Lip accumulated around angiogenic vessels, and APRPG-PEG-Lip associated with angiogenic vessels [15]. Therefore, we next determined the intratumoral distribution of the two liposomes by using confocal laser scan microscopy. On the other hand, biodistribution study showed the spleen and liver retention of liposomes. This retention is much lower than that of liposome without PEG-modification and the drug in them would show little effect on non-proliferative cells.

As shown in Fig. 3, APRPG-PEG-Lip and PEG-Lip were mainly distributed inside of vessel like structure after 2 h injection. Since these liposomes had long-circulating characteristics, they would effectively reach the vessel of the pancreatic tumor. Intravessel distribution of liposomes, however, was much different in these two kinds of liposomes. APRPG-PEG-Lip was colocalized with vessel marker CD31, although PEG-Lip was rather evenly distributed inside the vessel like structure. The accumulation of PEG-Lip at outside of vessels was not observed at this time point, although these vessels should be angiogenic vessels since APRPG-PEG-Lip having affinity to only neovessels associated with the vessels. The target of APRPG peptide is unclear at present, however, cellular uptake of APRPG-modified liposome significantly increased in VEGF-stimulated human umbilical vein endothelial cells (HUVECs) *in vitro* suggesting that some molecule which was expressed on the surface of the cells by the stimulation is responsible for the interaction. Moreover, a previous paper reported that one peptide including the PRP motif had an affinity for VEGF receptor [21]. Therefore, APRPG peptide may interact with endothelial cells through a certain molecule on the cell surface.

Finally, we examined the effect of ANET on the pancreatic tumor, and observed significant suppression of tumor growth by the treatment with APRPG-PEG-Lip encapsulating ADM. Since APRPG-PEG-Lip directly associated with growing angiogenic endothelial cells, ADM in the liposome might damage the angiogenic vessels. Generally, in pancreatic cancer, scirrhous gastric cancer and inflammatory breast cancer, drug carrier-based DDS require a long-distance transportation to get to the tumor cells which is a disadvantage for targeting DDS. PEG-Lip accumulated passively is thought to remain in large volume of stroma exists in pancreatic cancer, followed by poor anti-tumor activity. The APRPG-based anti-neovascular system may overcome this disadvantage by directly and effectively injuring targeted proliferative angiogenic vessels. Immunohistochemical analysis also supported the idea.

In conclusion, ANET has the possibility to treat hypovascular pancreatic tumor by injuring the neovessels. APRPG-modification of PEG-Lip endows it with binding ability to angiogenic endothelial cells, therefore ADM encapsulated in the liposome may effectively damage the cells, which causes enhanced therapeutic efficacy compared to that by ADM in PEG-Lip. Since PEG-Lip accumulated in orthotopic pancreatic tumor in a similar extent to APRPG-PEG-Lip, the inferior therapeutic efficacy of ADM in PEG-Lip to that in APRPG-PEG-Lip might be due to the topological distribution difference: PEG-Lip might reside in the interstitial spaces of the tumor, and gradually release ADM which causes damage of growing cells.

References

[1] A. Jemal, T. Murray, A. Samuels, A. Ghafoor, E. Ward, M.J. Thun, Cancer statistics, CA Cancer J. Clin. 53 (1) (2003) 5–26.
[2] D.R. Martin, R.C. Semelka, MR imaging of pancreatic masses, Magn. Reson. Imaging Clin. N. Am. 8 (4) (2000) 787–812.
[3] J. Rosai, in: J. Rosai (Ed.), Ackerman's Surgical Pathology, 8th ed, Mosby, St. Louis, 1996, pp. 969–1013.
[4] R.C. Semelka, L.L. Nagase, D. Armao, et al., in: R.C. Semelka (Ed.), Abdominal-Pelvic MRI, 2nd ed, Wiley–Liss, New York, 2002, pp. 373–490.
[5] C.J. Bruns, C.C. Solorzano, M.T. Harbison, S. Ozawa, R. Tsan, D. Fan, J. Abbruzzese, P. Traxler, E. Buchdunger, R. Radinsky, I.J. Fidler, Blockade of the epidermal growth factor receptor signaling by a novel tyrosine kinase inhibitor leads to apoptosis of endothelial cells and therapy of human pancreatic carcinoma, Cancer Res. 60 (11) (2000) 2926–2935.
[6] R.G. Chirivi, A. Garofalo, M.J. Crimmin, L.J. Bawden, A. Stoppacciaro, P.D. Brown, R. Giavazzi, Inhibition of the metastatic spread and growth of B16–BL6 murine melanoma by a synthetic matrix metalloproteinase inhibitor, Int. J. Cancer 58 (3) (1994) 460–464.
[7] S.A. Eccles, G.M. Box, W.J. Court, E.A. Bone, W. Thomas, P.D. Brown, Control of lymphatic and hematogenous metastasis of a rat mammary carcinoma by the matrix metalloproteinase inhibitor batimastat (BB-94), Cancer Res. 56 (12) (1996) 2815–2822.
[8] H. Hurwitz, L. Fehrenbacher, W. Novotny, T. Cartwright, J. Hainsworth, W. Heim, J. Berlin, A. Baron, S. Griffing, E. Holmgren, N. Ferrara, G. Fyfe, B. Rogers, R. Ross, F. Kabbinavar, Bevacizumab plus irinotecan, fluorouracil, and leucovorin for metastatic colorectal cancer, N. Engl. J. Med. 350 (23) (2004) 2335–2342.
[9] B.A. Teicher, N.P. Dupuis, M.F. Robinson, Y. Emi, D.A. Goff, Antiangiogenic treatment (TNP-470/minocycline) increases tissue levels of anticancer drugs in mice bearing Lewis lung carcinoma, Oncol. Res. 7 (5) (1995) 237–243.
[10] H. Satoh, H. Ishikawa, M. Fujimoto, M. Fujiwara, Y.T. Yamashita, T. Yazawa, M. Ohtsuka, S. Hasegawa, H. Kamma, Angiocytotoxic therapy in human non-small cell lung cancer cell lines-advantage of combined effects of TNP-470 and SN-38, Acta Oncol. 37 (1) (1998) 85–90.
[11] N. Oku, T. Asai, K. Watanabe, K. Kuromi, M. Nagatsuka, K. Kurohane, H. Kikkawa, K. Ogino, M. Tanaka, D. Ishikawa, H. Tsukada, M. Momose, J. Nakayama, T. Taki, Anti-neovascular therapy using novel peptides homing to angiogenic vessels, Oncogene 21 (17) (2002) 2662–2669.
[12] T. Asai, M. Nagatsuka, K. Kuromi, S. Yamakawa, K. Kurohane, K. Ogino, M. Tanaka, T. Taki, N. Oku, Suppression of tumor growth by novel peptides homing to tumor-derived new blood vessels, FEBS Lett. 510 (3) (2002) 206–210.

[13] N. Maeda, Y. Takeuchi, M. Takada, Y. Namba, N. Oku, Synthesis of angiogenesis-targeted peptide and hydrophobized polyethylene glycol conjugate, Bioorg. Med. Chem. Lett. 14 (4) (2004) 1015–1017.
[14] N. Maeda, Y. Takeuchi, M. Takada, Y. Sadzuka, Y. Namba, N. Oku, Anti-neovascular therapy by use of tumor neovasculature-targeted long-circulating liposome, J. Control. Release 100 (1) (2004) 41–52.
[15] N. Maeda, S. Miyazawa, K. Shimizu, T. Asai, S. Yonezawa, S. Kitazawa, Y. Namba, H. Tsukada, N. Oku, Enhancement of anticancer activity in antineovascular therapy is based on the intratumoral distribution of the active targeting carrier for anticancer drugs, Biol. Pharm. Bull. 29 (9) (2006) 1936–1940.
[16] C.H. Crane, L.M. Ellis, J.L. Abbruzzese, C. Amos, H.Q. Xiong, L. Ho, D.B. Evans, E.P. Tamm, C. Ng, P.W. Pisters, C. Charnsangavej, M.E. Delclos, M. O'Reilly, J.E. Lee, R.A. Wolff, Phase I trial evaluating the safety of bevacizumab with concurrent radiotherapy and capecitabine in locally advanced pancreatic cancer, J. Clin. Oncol. 24 (7) (2006) 1145–1151.
[17] H.L. Kindler, G. Friberg, D.A. Singh, G. Locker, S. Nattam, M. Kozloff, D.A. Taber, T. Karrison, A. Dachman, W.M. Stadler, E.E. Vokes, Phase II trial of bevacizumab plus gemcitabine in patients with advanced pancreatic cancer, J. Clin. Oncol. 23 (31) (2005) 8033–8040.
[18] N. Oku, Anticancer therapy using glucuronate modified long-circulating liposomes, Adv. Drug Deliv. Rev. 40 (1–2) (1999) 63–73.
[19] D.T. Auguste, R.K. Prud'homme, P.L. Ahl, P. Meers, J. Kohn, Association of hydrophobically-modified poly(ethylene glycol) with fusogenic liposomes, Biochim. Biophys. Acta 1616 (2) (2003) 184–195.
[20] H. Maeda, J. Wu, T. Sawa, Y. Matsumura, K. Hori, Tumor vascular permeability and the EPR effect in macromolecular therapeutics: a review, J. Control. Release 65 (1–2) (2000) 271–284.
[21] R.J. Giordano, M. Cardo-Vila, J. Lahdenranta, R. Pasqualini, W. Arap, Biopanning and rapid analysis of selective interactive ligands, Nat. Med. 7 (11) (2001) 1249–1253.

Increased Gene Expression by Cationic Liposomes (TFL-3) in Lung Metastases Following Intravenous Injection

Wenhao Li,[a] Tatsuhiro Ishida,[a] Yurie Okada,[a] Naoto Oku,[b] and Hiroshi Kiwada*,[a]

[a] *Department of Pharmacokinetics and Biopharmaceutics, Faculty of Pharmaceutical Sciences, The University of Tokushima; 1–78–1 Sho-machi, Tokushima 770–8505, Japan: and* [b] *Department of Medical Biochemistry and COE program in the 21st Century, University of Shizuoka School of Pharmaceutical Sciences; 52–1 Yada, Shizuoka 422–8526, Japan.* Received November 22, 2004; accepted January 13, 2005

We recently showed that size, not surface charge, is a major determinant of the *in vitro* lipofection efficiency of pDNA/TFL-3 complex (lipoplex), even in the presence of serum. In this study, the effect of lipoplex size as a result of interaction with serum proteins on *in vitro* lipofection and the relationship of this with *in vivo* lipofection was examined in a murine lung metastasis model. As previously described, the pDNA to lipid ratio (P/L ratio) affected both the size and zeta potential of the lipoplex. *In vitro* studies also indicated that transgene expression in B16BL6 cells was largely dependent on the size of the lipoplex, both in the absence or presence (50% (v/v)) of serum. An *in vivo* lipofection experiment showed that predominant gene expression in lungs occurred only in tumor-bearing mice, not in normal mice. Based on the *in vitro* study, this tumor-related gene expression was not related to lipoplex size in the presence of serum (50% (v/v)), suggesting that the size alteration, as the result of interactions with serum proteins in the blood stream may not play an important role in the case of systemic injections. In addition, the efficient gene expression in tumor-bearing lung was not related to the progression of lung metastases. The area-specific gene expression in tumor-bearing lungs, which was largely dependent on the P/L ratio of the lipoplexes, was observed by fluorescent microscopy. Although the underlying mechanism for the area-specific transgene expression is not clear, it may be related to the interaction of lipoplexes with tumor cells, vascular endothelial cells under angiogenesis and normal cells in the lungs. The possibility that TFL-3 is a useful utility to the targeted delivery of pDNA to lungs and tumor-related lipofection is demonstrated. This result suggests that area-specific gene expression in lung metastases may be achieved by controlling the physicochemical properties of the lipoplex, *i.e.* the P/L ratio.

Key words gene delivery; lipofection; lung metastasis; cationic liposome

Gene therapy, a promising medical technology against many diseases, has some potential for the treatment of certain types of serious cancer such as lung cancer.[1] During the past 15 years, more than 400 clinical studies in gene therapy have been evaluated and almost 70% of these studies were in the area of cancer gene therapy.[2,3] However, even though much clinical research has been carried, the validity of this treatment has not been confirmed.[4]

The key for successful gene therapy in the treatment of cancer is the technology used for gene delivery, in which targeted gene delivery to a tumor is achieved. For this purpose, many studies have been directed toward the development of a useful vector system. Vectors for gene therapy can be categorized into two groups: viral and non-viral vectors. The viral vectors mimic the properties of viruses that naturally infect cells and transfer their genetic materials, resulting in a highly efficient gene transfer. They have, however, some limitations which include difficulty for production and toxicity (in particular immunogenecity).[5] Non-viral vectors based on (poly)cationic lipids, liposomes, and polymers form negatively charged natural and synthetic DNA. It is generally believed that the positive charge on the vector/DNA complex ensures its binding to the cell membrane because of the negative charge on the cell membrane and it then enters the target cells. Although the gene transfer efficiency of non-viral vectors is less than that of their viral counterparts and is also transient in nature, these systems are likely to present several advantages including low-cost and large-scale production, safety, lower immunogenecity, and the capacity to deliver large gene fragments.

A cationic liposome, TFL-3, composed of a cationic lipid, DC-6-14, with helper lipids dioleoylphosphatidylethanolamine (DOPE) and cholesterol (CHOL), showed a higher lipofection efficiency in dividing or non-dividing cells *in vitro*, even in the presence of serum[6–8] and *in vivo*.[9] Generally, gene fragments in complexes formed with non-viral vectors are easily and quickly degraded in the presence of serum.[10] An electron microscopic study showed that gene fragments/TFL-3 complexes (lipoplexes) retained their morphology in the presence of serum.[6] This may account for the high gene transfer activity in serum-containing media and *in vivo*. Based on the above discussion, TFL-3 would be expected to be a superior non-viral vector that could be systemically injected.

In vivo lipofection, the transgene expression would occur as a function of the distribution of the lipoplexes. In addition to the physicochemical properties of the component lipids, the colloidal properties of lipoplexes such as their stability in plasma, pharmacokinetics and biodistribution are major determinant factors achieving the highest transgene and tissue specific expressions.[11–14] Organ distribution can be modulated by varying the lipid-to-pDNA ratio or the size of the lipoplexes.[15]

With the aging of society in the 21st century, the incidence of cancer is expected to increase. The morbidity rate of lung cancer has been rising particularly rapidly, and a pressing countermeasure is necessary.[16] Lipoplexes usually accumulate largely in the lung, although the distribution changes with time: lipoplexes are found in the lung shortly after intravenous injection but eventually accumulate in the liver after 24 or 48 h.[17,18] This is because the lipoplex form aggregates in the blood stream, and is captured in the first capillary en-

* To whom correspondence should be addressed. e-mail: hkiwada@tokushima-u.ac.jp

countered. If the pDNA could be quickly transferred from lipoplexes to pulmonary endothelial cells after being captured in a capillary of the lung, an enhanced transgene expression might be obtained. In a lung with a tumor, a more extensive gene expression would be observed because of the angiogenesis of vessels and the proliferation of cells in the tumor area.

The focus of this study, therefore, was on the *in vitro* characterization of lipoplexes (pDNA/TFL-3 complex) and the relationship between their characteristics and *in vitro* or *in vivo* transgene expression. For this purpose, we employed a line of highly lung-metastatic melanoma cells, B16BL6, to study *in vitro* transgene expression efficiency and a murine lung metastatis model to examine *in vivo* efficiency.

MATERIALS AND METHODS

Materials TFL-3 composed of *O,O'*-ditetradecanoyl-*N*-(α-trimethylammonioacetyl) diethanolamine chloride/DOPE/CHOL (1/0.75/0.75, mol/mol) was a generous gift from the Daiichi Pharmaceutical Co. Ltd. (Tokyo, Japan). The luciferase assay kit and cell culture lysis reagent (CCLR) were purchased from Promega (WI, U.S.A.). Plasmid DNA (pDNA) pCAG-Luc3 encoding the firefly luciferase, was purchased from Nippon Gene (Toyama, Japan). A pDNA encoding the green fluorescence protein (GFP) gene, gWIZ-GFP was obtained from Gene Therapy Systems, Inc (CA, U.S.A.). pDNA was amplified in E. Coli JM 109 and purified by means of a QIAfilter Plasmid Mega Kit from Qiagen (Hilden, Germeny). LipofectAMINE was purchased from Invitrogen (CA, U.S.A.). Fetal bovine serum (FBS) was purchased from GIBCO BRL (NY, U.S.A.). Opti-MEM I medium was purchased from Life Technologies (MD, U.S.A.). Other cell culture regents were obtained from Nissui Pharmaceutical Co. Ltd. (Tokyo, Japan). All other reagents were of analytical grade.

Cell Line and Animal B16BL6, a murine melanoma cell line, was cultured in DMEM medium supplemented with 10% heat-inactivated FBS, 10 mM glutamine, 100 units/ml penicillin, and 100 μg/ml streptomycin in a 5% CO_2 air incubator at 37 °C. Six-week-old male C57BL6 mice, 20—22 g in weight, were purchased from Japan SLC (Shizuoka, Japan). They had free access to water and rat chow, and were housed under controlled environmental conditions (constant temperature, humidity, and a 12 h dark–light cycle). All animal experiments were evaluated and approved by the Animal and Ethics Review Committee of Faculty of Pharmaceutical Sciences, The University of Tokushima.

Preparation of pDNA/TFL-3 Complex (Lipoplex) Lipoplex was prepared by gently mixing the appropriate amount of pDNA into TFL-3 with different lipid concentrations (2.5 μM or 25 μM) to obtain the desired pDNA to lipid ratio. The pDNA to lipid (P/L) ratio was varied from 0 to 150 g pDNA per total lipid (mol) in liposomes, corresponding to a mol ratio of 0—2.8×10^{-5}. The lower lipid concentration was for *in vitro* use and the higher concentration was for *in vivo* use.

Characterization of the Lipoplex The particle size and zeta-potential of the resulting lipoplex in 9% sucrose solution with or without 50% (v/v) serum were determined using a laser particle analyzer and a laser electrophoresis zeta potential analyzer device, NICOMP 380 (Particle sizing system, CA, U.S.A.).

In Vitro* Transfection** B16BL6 cells were plated in 12-well plates at a density of 1.5×10^5 cells/well. After an over night pre-culture, the first 200 μl of Opti MEM or serum was added to a well of a 12-well plate, then 200 μl of lipoplex (2.5 μg pDNA/ml) was immediately added. After 1 h of lipofection, the lipoplex was removed and the wells were washed twice with cold phosphate buffered saline (PBS, pH 7.4). Appropriate medium supplemented with 10% heat-inactivated FBS was then added and the cells were cultured for a further 23 h. For the luciferase assay, after removal of the medium, the cells were lysed by the addition of 400 μl of CCLR. The cell lysate was collected and centrifuged (2 min, 20000×g***, 4 °C) to give a clear supernatant for the assay. The luciferase assay was carried out according to the manufacturer's recommended protocol (Promega, WI, U.S.A.). The protein content in the clear supernatant was determined with a DC protein assay kit (Bio-Rad Laboratories, CA, U.S.A.). The data are expressed as light counts/min/mg of protein.

In Vivo* Transfection** To induce pulmonary metastases, murine B16BL6 melanoma cells (5×10^4 cells/mouse) were intravenously injected with 0.2 ml of PBS(−) *via* the tail vein of a C57BL/6 mouse. At the indicated day after the inoculation, lipoplex was intravenously injected *via* the tail vein. The dose of pDNA for injection was fixed at 30 μg. At 24 h after the injection, the lungs were removed from the mouse. To dissect, the lung was homogenized followed by three freeze-thaw cycles in 1 ml of CCLR. The resulting tissue homogenate was then centrifuged (10 min, 20000×g***, 4 °C). The clear supernatant was subjected to the luciferase assay as described above.

Fluorescent Microscopic Study Lipoplex containing pDNA encoding the green fluorescence protein (GFP) gene, gWIZ-GFP (30 μg pDNA/mouse), was intravenously injected into a B16BL6-bearing mouse *via* the tail vein. At 24 h after *in vivo* lipofection, the lungs were removed from the mice, immediately embedded in 4% CMC embedding compound (FINETEC Co., Ltd., Tokyo, Japan), frozen in liquid nitrogen, and stored at −80 °C. Frozen lung sections (100 μm thick) were made using a cryostat by the routine procedure. The sections were directly examined using a Zeiss LSM5 inverted confocal laser scan microscope (Carl Zeiss, Germany) without any fixation. GFP was imaged using 488 nm for excitation and 510—530 nm for emission.

Statistics All mean values are expressed as the mean±S.D. Statistical analyses were performed using GraphPad InStat software (GraphPad Software, CA, U.S.A.). The level of significance was set at $p<0.05$.

RESULTS

Effect of P/L Ratio on Size, Zeta Potential and Transfection Efficiency of the Lipoplex The size of the lipoplex was examined for varying ratios of pDNA to lipid of TFL-3 liposomes (P/L ratio) in the absence of serum (Fig. 1A). The mean size of the original TFL-3 before preparation of the lipoplex was approximately 150 nm. Complexing of liposomes with an increasing amount of pDNA, up to 80 P/L ratio, resulted in a dramatic increase in the size of lipoplex. At a P/L ratio of 80, the largest size lipoplex was obtained.

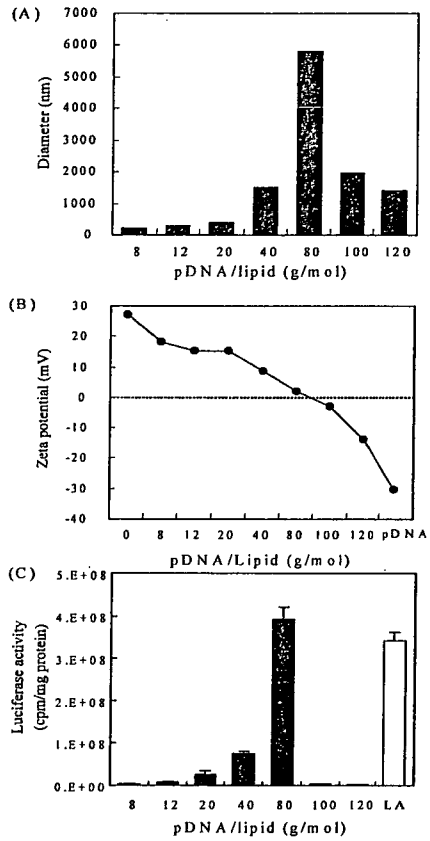

Fig. 1. Effect of P/L Ratio on Size, Zeta Potential and Transfection Efficiency of the Lipoplex

pDNA/TFL-3 complexes (lipoplexes) were prepared, as described method in Materials and Methods. The average size (A) and zeta-potential (B) of the resulting lipoplex were determined. Luciferase activity (C) in B16BL6 cells following lipofection (1 μg of pDNA) was determined, as described in Materials and Methods. Filled column, pDNA/TFL-3 complex; open column, pDNA/LipofecAMINE (LA) complex. Data represent mean±S.D. (n=3).

This can be attributed to extensive, uncontrolled aggregation and fusion between lipoplexes due to their loss of surface charge. Conversely, the complexing of greater amounts of pDNA with liposomes resulted in a decrease in size.

Complexing of an increasing amount of pDNA with cationic liposomes led to a decrease in the initial zeta potential value of the liposome (approximately +28 mV) (Fig. 1B). Lipoplex with a 80 P/L ratio, which has a neutral calculated charge, had almost a neutral in a zeta potential measument (approximately +2 mV). A further increase in the amount of pDNA in the lipoplex resulted in net negative zeta potentials.

B16BL6 cells were transfected using lipoplexes prepared with different P/L ratios. The transgene efficiency of the lipoplex changed dramatically with a change in P/L ratio (Fig. 1C). A lipoplex, at 80 P/L ratio, showed the highest efficiency, almost same as that of LipofectAMINE, which was used as positive control. At this ratio, the size of the lipoplex was at a maximum, but had almost a neutral charge. The lower lipofection efficiencies of all other lipoplexes were not due to cytotoxicity toward the treated cells, since all the lipoplexes tested showed no detectable cytotoxicity, as evidenced by the trypan blue exclusion test (data not shown).

Effect of P/L Ratio on Lipoplex Size and Transfection Efficiency in the Presence of Serum It is well known that

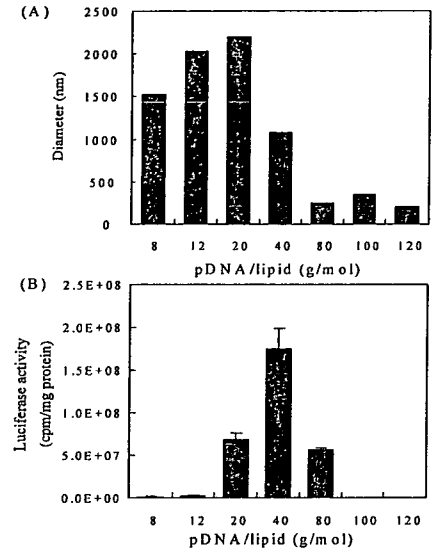

Fig. 2. Effect of P/L Ratio on Size and Transfection Efficiency of the Lipoplex in the Presence of Serum

pDNA/TFL-3 complexes (lipoplexes) were prepared, as described in Materials and Methods. The average size (A) of resulting lipoplex were determined after incubation in the presence of 50% (v/v) serum for 15 min at 37 °C. Luciferase activity (B) in B16BL6 cells following lipofection (1 μg of pDNA) was determined in the presence of 50% (v/v) serum according to the method described in the Materials and Methods. Data represent mean±S.D. (n=3).

serum has an inhibitory effect on lipofection efficiency. After its systemic administration, the lipoplex immediately encounters serum proteins in the blood stream. Hence, a study in the presence of serum is thought to be very important for the prediction of lipofection efficiency *in vivo*. Here, the effect of serum was investigated on lipoplex size and lipofection efficiency. For all experiments, the concentration of serum was fixed at 50% (v/v) in the incubation medium.

As expected, the presence of serum resulted in a dramatic alteration in lipoplex size compared to the absence of serum (Fig. 2A). The P/L ratio needed to give the largest lipoplex size was shifted from 80 to 20 in the presence of serum, compared with the absence of serum. Up to a P/L ratio of 40, the size was increased 6 to 7-fold, relative to the absence of serum. Increasing the P/L ratio to over 40 led to a significant decrease in lipoplex size, 7 to 25-fold. In the presence of serum, the lipofection efficacy of the lipoplex on B16BL6 cells was also changed dramatically with a change in P/L ratio (Fig. 2B) and the P/L ratio for the maximum transgene expression was shifted from 80 to 40 P/L. The level of gene expression was relatively lower than those in the absence of serum, except for P/L ratios of 20 and 40 (Fig. 2B). At P/L ratios of 20 and 40, transgene expression was increased by approximately 2-fold. LipofectAMINE lost its efficient gene transfer activity in the presence of serum (data not shown). Comparing the changes in lipoplex size and lipofection efficiency, a relationship still partly exists between lipoplex size and lipofection efficiency in the presence of serum.

***In Vivo* Transfection Study** The *in vivo* efficacy of lipoplex was examined in B16BL6-bearing mice, following an intravenous injection. The assay was carried out 14 d after the inoculation of B16BL6 cells or an injection of saline. In normal mice, a relatively lower gene expression in all organs including the lungs (Fig. 3, open column) examined were detected at all P/L ratios tested (data not shown). Surprisingly,

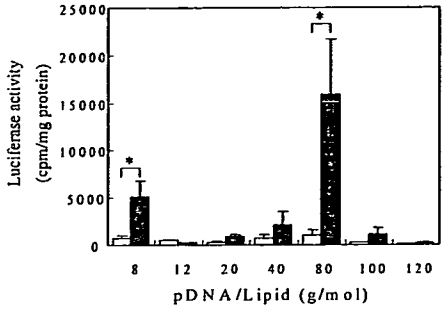

Fig. 3. Effect of P/L Ratio of the Lipoplex on Gene Expression in Lungs of Normal and B16BL6 Tumor-Bearing Mice

Lipoplexes, prepared as described in Materials and Methods, were intravenously injected in normal mice or tumor bearing mice at 14 d post-inoculation of B16BL6 cells. Each mouse received 30 μg of pDNA. The lungs of the animals were harvested 24 h after injection. The luciferase activity in the lungs was determined, as described in Materials and Methods, 24 h after lipoplex injection. Open column, normal mouse; filled column, tumor-bearing mouse. Data represent the mean±S.D. (n=4).

in tumor-bearing mice, a relatively higher gene expression in the lungs was obtained at several P/L ratios, whereas gene expression in various another organs was very low or absent (data not shown). The rank order of increased gene expression level was for P/L ratios of 80, 8, 40, 100 and 20. The tendency observed in tumor-bearing mice reflects the *in vitro* lipofection results obtained in the absence of serum rather than those in the presence of serum.

To further examine the *in vivo* transfection efficiency, the lipoplex was intravenously injected into tumor-bearing mice at the indicated days after tumor cell inoculation. Gene expression in the lung was assayed 24 h after lipoplex injection. Two different lipoplexes with P/L ratios of 8 and 80, which showed relatively higher transgene expression (Fig. 3), were used in this study. The progression of tumor in lung was estimated by counting the number of tumor nodules on the surface of the lung. As shown in Fig. 4A, the extensive progression of tumor was not observed until at 14—15 d after tumor cell inoculation. For both lipoplexes, while tumor bearing mice showed no significant gene expression at earlier periods (until 7 d after tumor inoculation), they showed significant gene expression at a later period (over 10 d after tumor inoculation) (Fig. 4B). With the lipoplex (8 P/L ratio), significant gene expression occurred when the lipoplex was administered at 10 d after tumor inoculation, then reached a maximum at 14 d and remained constant even at 17 and 21 d. In the case of the lipoplex (80 P/L ratio), significant gene expression occurred when the lipoplex was given at 10 d after tumor inoculation, reached a maximum level at 14 d and then decreased almost to the control level up to 21 d. The level of gene expression by the lipoplex with a 80 P/L ratio was 2-times higher than that for the lipoplex with a 8 P/L ratio at earlier after tumor inoculation, but this value became 8-times lower later. There was no obvious relation between the gene expression induced by TFL-3 and the number of tumor nodules in the lung.

Fluorescence Microscopic Study of Lung The lipoplex (gWIZ-GFP/ TFL-3) with a P/L ratio of 8 or 80 was intravenously injected into tumor-bearing mice at 14 d post-tumor inoculation. In the normal lung, GFP expression was observed in endothelial cells of the microvasculature and there was no significant difference in the area of GFP expression with both lipoplexes tested (data not shown). In the tumor-

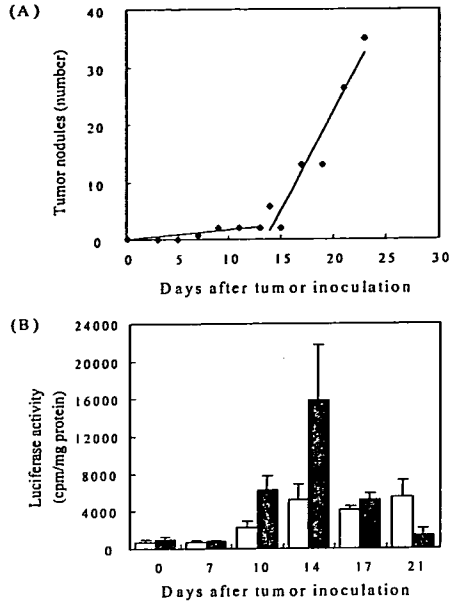

Fig. 4. Relation between Tumor Progression and Gene Expression in Lungs

(A) B16BL6 cells (5×10^4 cells in 0.2 ml PBS) were intravenously injected into a C57BL/6 mouse. At the indicated day, the mice were sacrificed. The number of tumor nodules on the surface of the lung was counted. (B) At the indicated day post-tumor inoculation, the lipoplex with a P/L ratio of 8 or 80 (30 μg of pDNA) was injected intravenously. The luciferase activity in the lungs was determined as described in Materials and Methods 24 h after lipoplex injection. Open column, lipoplex of 8 P/L ratio; filled column, lipoplex of 80 P/L ratio. Data represent the mean±S.D. (n=4).

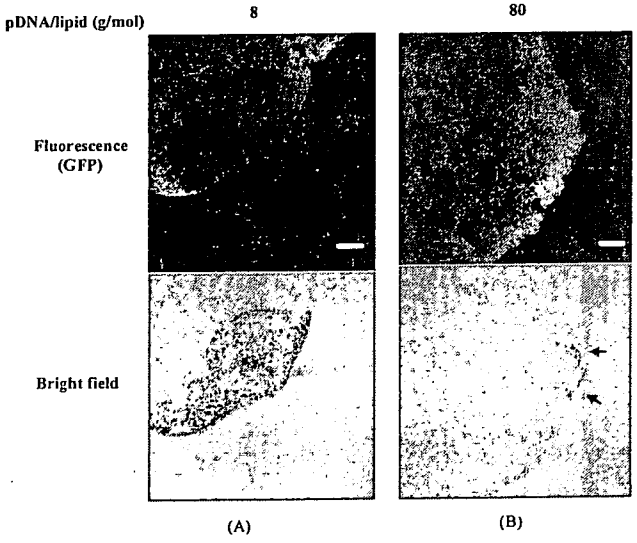

Fig. 5. Fluorescent Microscopic Observation of Expressed GFP in the Tumor-Bearing Lung

At 14 d post-tumor inoculation, the lipoplex with a P/L ratio of 8 or 80 (30 μg of pDNA) was injected intravenously. At 24 h after injection, GFP expression in the lungs was observed under a confocal laser scan microscope as described in Materials and Methods. In the left picture (A), the dark area in the bright field represents tumors in the prepared section. In the right picture (B), the black arrow heads represents very tiny tumors in the prepared section. The scale bar in the pictures represents 100 μm. The pictures shown are typical examples of multiple evaluations.

bearing lung, with the lipoplex with a P/L ratio of 8, the expressed GFP was barely detected in the tumor area (Fig. 5A). Interestingly, the strongest GFP expression was observed in the tissue around the tumor. In contrast to this observation, with the lipoplex with a P/L ratio of 80, the expressed GFP

was detected in the entire lung tissue unrelated to the area of tumor growth (Fig. 5B).

DISCUSSION

Many parameters are known to affect the efficiency of transfection by lipoplex (lipofection) *in vitro* and *in vivo*. Among these parameters, one of factors that affect lung lipofection is the interaction of lipoplex with serum. It has been reported that incubation in pure serum or serum-containing media could decrease the extent of lipoplex delivery and alter its intracellular fate[19,20] and even cause the lipoplex to disintegrate upon prolonged exposure.[18,21] However, an injected lipoplex is rapidly cleared from the circulation[18,22] and internalized in the lungs,[23] thus ruling out long-term exposure to serum. In addition, Sakurai *et al.* showed the pre-incubation of a DOTAP/Chol lipoplex with serum for as long as 30 min did not significantly impair lipofection in the lungs.[24] Accordingly, the importance of the above mentioned serum effects for lung tansgene expression following intravenous injection of lipoplex is still an open question.

Our earlier study showed that the size of lipoplex is a major determinant in the lipofection efficiency of TFL-3 in the presence of serum with A431, a human epidermoid carcinoma cell line, and SBC-3, a human lung cancer cell line.[25] Therefore, in this study, we focused on the effect of lipoplex size as the result of from interaction with serum proteins on *in vitro* lipofection and on their relation with *in vivo* lipofection in tumor-bearing mice. As shown in Figs. 1 and 2, the importance of lipoplex size was also confirmed in *in vitro* lipofection with B16BL6 cells in the absence or presence of serum. Interestingly, in the presence of serum, the size of lipoplex that has over P/L ratio of 40 was decreased relative to absence of serum (Figs. 1A, 2A). This may result from that the larger lipoplex as a result of aggregation of smaller lipoplexes was dispersed by the interposition of serum proteins.[10] The *in vitro* lipofection of the lipoplex in the presence of serum (Fig. 2) showed no obvious relation with *in vivo* lipofection in tumor-bearing mice (Fig. 3). Probably, the alteration in the size of lipoplex, resulted from aggregate formulation with anionic serum proteins after intravenous injection, is not a major factor in determining *in vivo* lipofection efficiency in our system. Otherwise, an interaction with serum proteins would not lead to a predominant change in the size of the lipoplex after an intravenous injection. During the intravenous injection of lipoplex, the lipoplex mixes with about 50—100 μl of serum, presuming cardiac flow through the tail vein and abdominal veins to be *ca.* 300 μl of serum per 3 s.[26] In this situation, *i.e.* 50—100 μl serum/200 μl of lipoplex dispersion, the serum concentration is much considerably diluted compared with our *in vitro* experimental conditions (50% (v/v)). In the presumed *in vivo* condition, at the lipoplex/serum ratio, the cationic membrane surfaces are only partially associated with anionic serum proteins, which therefore may not act as bridges between lipoplexes, thereby not inducing lipoplex aggregation well.

Previous studies using TFL-3 showed a high transfection efficiency *in vitro*, even in the presence of serum, and *in vivo* a low toxicity was reported by intraperitoneal injection.[9] Accordingly, TFL-3 would be expected to be applicable for *in vivo* use with systemic injection. Here, we report that tumor-related gene expression in the lung is achieved by using TFL-3 (Fig. 3). In our artificial metastasis model of murine melanoma, some micrometastases were established in the lung due to the direct intravenous injection of the cells. Once established, the pulmonary metastases secrete factors that promote angiogenesis and then begin to proliferate progressive, resulting in an enlarged vascular bed and an increase in vascular permeability. Simberg *et al.*[27] recently reported that hypervascularization in the liver induced by VEGF did not increase level of lipofection with a DOTAP/CHOL lipoplex, despite the increased entrapment of lipoplex in the liver. Based on the fact that enlarging the vascular bed and increasing vascular permeability in the liver were not sufficient to promote efficient lipofection, they concluded that the lungs might be an organ that is simply susceptible than liver. Accordingly, the predominant tumor-related gene expression in this study may have been obtained due to the following reasons: (a) the lung is a more lipofectable organ, (b) hypervascularization occurred due to tumor progression, and (c) extensive proliferation of tumor cells occurred. But, we can not exclude influence of alteration of biological conditions related to tumor progression on the resulting gene expression in the lung.

The P/L ratio of a lipoplex of TFL-3 affected the degree of gene expression in tumor-bearing lungs (Fig. 3). In addition, pulmonary gene expression was dependent on the time after tumor cell inoculation (Fig. 4). These observations lead to the possibility that the lipoplex causes gene expression in a different part of the lung. This area-specific gene expression may be related, in part, to the pattern of interaction of lipoplexes with tumor cells, pulmonary endothelial cells and normal cells. To assess this, a fluorescent microscopic study was carried out. The findings showed that the lipoplex with a P/L ratio of 8 expressed GFP over the surrounding tumor cells, while the lipoplex, with a P/L ratio of 80, expressed it in the entire lung tissue without any specificity (Fig. 5). The first pass entrapment (60—80% of the liposomes are entrapped within minutes after intravenous injection)[18,22,28] can be attributed to the highly extended lung capillary bed and was proposed to explain the predominant gene expression in the lungs.[28,29] Ito *et al.*[30] recently reported that vascular endothelial cells, probably under angiogenesis, in the lungs of tumor bearing mice, which demonstrates an increased uptake of cationic liposome–DNA complexes and transgene expression compared to normal mice. In addition, they showed that the increased uptake of liposome–DNA complexes by tumor cells over normal cells is also responsible for the increased transgene expression. The alveolar macrophages present in a tumor microenvironment could be less responsible for the transgene expression, since it has been reported that macrophages are less phagocytic or are inactivated by factors produced by the tumor cells.[31,32] Accordingly, the P/L ratios of lipoplexes showing the largest difference in physicochemical properties, as shown in Figs. 1 and 2, affect the microdistribution of lipoplexes, their interaction with various cells and uptake by those cells after intravenous injection, may result in the area-specific gene expression in tumor-bearing lungs.

Although the present study demonstrates that the increased gene expression in tumor-bearing lungs is probably due to an increased uptake of lipoplex by tumor cells and pulmonary

endothelial cells of normal or angiogenic vessels over the surrounding normal cells, it is possible that other factors such as endosomal release, nuclear uptake, and increased transcription and translation, may play a role in the different degree and distribution pattern observed for gene expression in the lung. A further examination of these individual phenomena may aid in the development of an effective gene delivery vector. However, a note of caution is that the experimental metastases model used in this study, although performed in such a way that the lung metastases are established, has some limitations. It does not mimic the full sequence of events that primary tumors undergo. These cancer cells may undergo additional changes. Thus, it may not be predictive of the responses of these tumors to a systemically delivered gene therapy agent. Therefore, the results of the present study, although relevant for lung cancer therapy, represent only an intermediate step on the path toward the development of a systemic gene transfer with a broad utility.

Acknowledgements We thank Mr. Kenji Irimura, Drug Safety Research Laboratory, Taiho Pharmaceutics, for preparation of histopathological slide of lung. We wish to thank Dr. Hiroshi Kikuchi, Daiichi Pharmaceuticals, for helpful suggestions and Dr. Milton S. Feather for his helpful advice in writing the English manuscript. This study was supported, in part, by research grants from the Japanese Clinical Oncology Fund and the Osaka Cancer Research Foundation.

REFERENCES

1) Crystal R. G., *Science*, **270**, 404—410 (1995).
2) Edelstein M. L., Abedi M. R., Wixon J., Edelstein R. M., *J. Gene Med.*, **6**, 597—602 (2004).
3) Hughes R. M., *J. Surg. Oncol.*, **85**, 28—35 (2004).
4) Nathwani A. C., Benjamin R., Nienhuis A. W., Davidoff A. M., *Vox Sang.*, **87**, 73—81 (2004).
5) Temin H. M., *Hum. Gene Ther.*, **1**, 111—123 (1990).
6) Serikawa T., Suzuki N., Kikuchi H., Tanaka K., Kitagawa T., *Biochim. Biophys. Acta*, **1467**, 419—430 (2000).
7) Nguyen L. T., Ishida T., Ukitsu S., Li W. H., Tachibana R., Kiwada H., *Biol. Pharm. Bull.*, **26**, 880—885 (2003).
8) Li W., Ishida T., Tachibana R., Almofti M. R., Wang X., Kiwada H., *Int. J. Pharm.*, **276**, 67—74 (2004).
9) Kikuchi A., Aoki Y., Sugaya S., Serikawa T., Takakuwa K., Tanaka K., Suzuki N., Kikuchi H., *Hum. Gene Ther.*, **10**, 947—955 (1999).
10) Lew D., Parker S. E., Latimer T., Abai A. M., Kuwahara-Rundell A., Doh S. G., Yang Z. Y., Laface D., Gromkowski S. H., Nabel G. J., *Hum. Gene Ther.*, **6**, 553—564 (1995).
11) Tranchant I., Thompson B., Nicolazzi C., Mignet N., Scherman D., *J. Gene Med.*, **6** (Suppl. 1), S24—35 (2004).
12) Song Y. K., Liu F., Chu S., Liu D., *Hum. Gene Ther.*, **8**, 1585—1594 (1997).
13) Takakura Y., Nishikawa M., Yamashita F., Hashida M., *J. Drug Target.*, **10**, 99—104 (2002).
14) Dass C. R., *Int. J. Pharm.*, **267**, 1—12 (2003).
15) Templeton N. S., Lasic D. D., Frederik P. M., Strey H. H., Roberts D. D., Pavlakis G. N., *Nat. Biotechnol.*, **15**, 647—652 (1997).
16) Ries L. A., Wingo P. A., Miller D. S., Howe H. L., Weir H. K., Rosenberg H. M., Vernon S. W., Cronin K., Edwards B. K., *Cancer*, **88**, 2398—2424 (2000).
17) Parker S. E., Ducharme S., Norman J., Wheeler C. J., *Hum. Gene Ther.*, **8**, 393—401 (1997).
18) Niven R., Pearlman R., Wedeking T., Mackeigan J., Noker P., Simpson-Herren L., Smith J. G., *J. Pharm. Sci.*, **87**, 1292—1299 (1998).
19) Escriou V., Ciolina C., Lacroix F., Byk G., Scherman D., Wils P., *Biochim. Biophys. Acta*, **1368**, 276—288 (1998).
20) Yang J., Chen S., Huang L., Michalopoulos G. K., Liu Y., *Hepatology*, **33**, 848—859 (2001).
21) Zelphati O., Uyechi L. S., Barron L. G., Szoka F. C., Jr., *Biochim. Biophys. Acta*, **1390**, 119—133 (1998).
22) Mahato R. I., Anwer K., Tagliaferri F., Meaney C., Leonard P., Wadhwa M. S., Logan M., French M., Rolland A., *Hum. Gene Ther.*, **9**, 2083—2099 (1998).
23) Barron L. G., Gagne L., Szoka F. C., Jr., *Hum. Gene Ther.*, **10**, 1683—1694 (1999).
24) Sakurai F., Nishioka T., Saito H., Baba T., Okuda A., Matsumoto O., Taga T., Yamashita F., Takakura Y., Hashida M., *Gene Ther.*, **8**, 677—686 (2001).
25) Almofti M. R., Harashima H., Shinohara Y., Almofti A., Li W., Kiwada H., *Mol. Membr. Biol.*, **20**, 35—43 (2003).
26) Davies B., Morris T., *Pharm. Res.*, **10**, 1093—1095 (1993).
27) Simberg D., Weisman S., Talmon Y., Faerman A., Shoshani T., Barenholz Y., *J. Biol. Chem.*, **278**, 39858—39865 (2003).
28) Li S., Tseng W. C., Stolz D. B., Wu S. P., Watkins S. C., Huang L., *Gene Ther.*, **6**, 585—594 (1999).
29) Song Y. K., Liu F., Liu D., *Gene Ther.*, **5**, 1531—1537 (1998).
30) Ito I., Began G., Mohiuddin I., Saeki T., Saito Y., Branch C. D., Vaporciyan A., Stephens L. C., Yen N., Roth J. A., Ramesh R., *Mol. Ther.*, **7**, 409—418 (2003).
31) Sotomayor E. M., Fu Y. X., Lopez-Cepero M., Herbert L., Jimenez J. J., Albarracin C., Lopez D. M., *J. Immunol.*, **147**, 2816—2823 (1991).
32) Lopez D. M., Handel-Fernandez M. E., Cheng X., Charyulu V., Herbert L. M., Dinapoli M. R., Calderon C. L., *Anticancer Res.*, **16**, 3923—3929 (1996).

Gene Expression in Primary Cultured Mouse Hepatocytes with a Cationic Liposomal Vector, TFL-3: Comparison with Rat Hepatocytes

Lap Thi NGUYEN, Tatsuhiro ISHIDA, and Hiroshi KIWADA*

Department of Pharmacokinetics and Biopharmaceutics, Faculty of Pharmaceutical Sciences, The University of Tokushima; 1–78–1 Sho-machi, Tokushima 770–8505, Japan.
Received February 21, 2005; accepted April 28, 2005; published online May 11, 2005

We recently reported that a cationic liposomal vector, TFL-3, could be used to achieve significant gene expression in primary cultured rat hepatocytes (Nguyen *et al.*, *Biol. Pharm. Bull.*, 26, 880–885 (2003)). A combination of hepatocyte transplantation and hepatocyte-targeted gene transfer represents a potentially important strategy for expanding treatment options for liver disease. A widely applied approach to support cross-species is necessary before human applications can be realized. Therefore, in this study, we examined the utility of TFL-3 in another species of rodent hepatocytes, namely mouse hepatocytes. Gene expression in mouse hepatocytes by TFL-3 was successful and the level was higher than those in rat hepatocytes that we recently reported on. Interestingly, it appears that both the degree and rate of gene expression were dependent on the incubation time prior to lipofection as well as on the density of cells per dish, but these parameters were independent of the amount of pDNA associated with the cells. These significantly suggest that the culture time prior to and following lipofection, which are related to the biological condition of the cells, may be one of major factors that affect gene expression in hepatocytes and non- or less dividing cells.

Key words gene delivery; cationic liposome; hepatocyte; non-dividing cell; plasmid quantification

The liver is an important target organ for gene therapy, because hepatocytes synthesize a wide variety of proteins, perform a variety of post-translational modifications, and are involved in numerous diseases. Therefore, hepatocyte-targeted gene transfer would represent an important strategy for expanding treatment options for liver diseases. The successful gene expression in mouse hepatocytes in living animals was recently achieved by a rapid injection of a large amount of naked pDNA into a mouse tail vein (the hydrodynamics-based procedure).[1,2] Despite the many desirable features of the procedure such as simplicity, convenience, and high efficiency, this procedure is not suitable for the treatment of liver disease because it seriously damage the hepatocytes.[2,3]

We recently reported that a cationic liposomal vector, TFL-3[4] composed of a cationic lipid, DC-6-14, with helper lipids dioleoylphosphatidylethanolamine and cholesterol (1 : 0.75 : 0.75 molar ratio), achieved sufficient gene expression in primary cultured rat hepatocytes.[5] Hence, TFL-3 may be a suitable vector system for successful gene expression in hepatocytes and it may be an attractive candidate for use in *in vivo* or *ex vivo* gene therapy.

Among the currently available therapeutic options, hepatocyte transplantation is a promising procedure that could replace liver transplantation because it would overcome the shortage of available donors as well as a variety of technical difficulties.[6—9] Therefore, a combination of hepatocyte transplantation and *in vitro* hepatocyte-targeted gene transfer using TFL-3, leading to the efficient expression of functional proteins, such as enzymes or growth factors, represent an important strategy for expanding the treatment options for liver disease. However, a widely applied approach to support cross-species is needed before human applications: the utility of TFL-3 on gene expression in non-dividing mammalian cells should be tested with different species. Therefore, in this study, we further examined the utility of TFL-3 on transgene expression in another rodent hepatocyte, namely primary cultured mouse hepatocytes.

MATERIALS AND METHODS

Materials TFL-3 was a generous gift from Daiichi Pharmaceutical Co. Ltd. (Tokyo, Japan). The pDNA, pGL3- Control, encoding luciferase was purchased from Promega (WI, U.S.A.). Collagenase TYPE I was purchased from Funakoshi (Tokyo, Japan). Cell culture reagents were obtained from Nissui Pharmaceutical Co. Ltd., (Tokyo, Japan). Other reagents were of analytical grade. LipofectAMINE was purchased from Life Technologies (MD, U.S.A.).

Cell Preparation and Culture Parenchymal hepatocytes were isolated from an adult male 4 ddY mouse weighing 17—22 g (Japan SLC, Shizuoka, Japan) or adult male Wistar rats weighing 170—200 g (Japan SLC, Shizuoka, Japan) using the in situ perfusion method, as described earlier.[5,10] Animal experiments were evaluated and approved by the Animal and Ethics Review Committee of Faculty of Pharmaceutical Sciences, The University of Tokushima. The isolated hepatocytes were plated at a density of 0.75×10^6 or 1.5×10^6 cells in 60 mm diameter collagen type I coated dish (IWAKI, Tokyo, Japan), and cultured at 37 °C under an atmosphere of humidified 5% CO_2 for 4 h to allow the cells to adhere to the dish. In each preparation, the viability of isolated cells was checked by trypan blue dye exclusion.

Lipofection and Luciferase Assay Lipofection was carried out using procedures as described in our earlier paper.[5] Briefly, pDNA/TFL-3 complexes were prepared at a ratio of 3 μg of pDNA to 30 nmol of cationic lipid. If necessary, rhodamine-labeled phosphatidylethanolamine (0.2% (mol/mol)) (Molecular probe, OR, U.S.A.) was incorporated in the liposome as a marker. At 18 or 42 h following the 4 h of preculture, the complexes were added to the dish at a final concentration of 1 μg pDNA/ml of media, which contained 5% heat-inactivated FBS (lipofection). After a 4 h lipofection period, the cells were further incubated in complete media for various times until used in the assays.

Luciferase activity was determined by a previously re-

* To whom correspondence should be addressed. e-mail: hkiwada@ph.tokushima-u.ac.jp

ported.[5] Briefly, the cells were lysed by the addition of 900 μl of cell culture lysis reagent (CCLR, Promega). An aliquot of the cell lysate was removed and the luciferase activity determined according to the manufacture's recommended protocol (Promega). The protein content of the lysate was measured with a DC protein assay kit (Bio-Rad Laboratories, CA, U.S.A.) and the data are represented as light counts/min/μg of protein.

Measurement of pDNA Delivered in the Hepatocytes The pDNA delivered to hepatocytes was quantitatively determined by using a method recently developed in our laboratory[11] with minor modifications. Briefly, at various times post-lipofection, the cells were suspended in 0.5 ml of lysis buffer (0.5% Nonidet P-40, 10 mM Tris, 10 mM NaCl, 3 mM $MgCl_2$, pH 7.4) to destabilize the plasma membrane. Aliquots of the suspension were subjected to PCR study. To extract intracellular DNA (containing pDNA), proteinase K (Merck, Frankfurter, Germany) was added to the fraction to a final concentration of 0.1 mg/ml. After an overnight incubation at 37 °C, proteins were eliminated by phenol/chloroform treatment; and the DNA was precipitated by the addition of ethanol. The precipitate was dissolved in TE buffer (10 mM Tris–HCl, 1 mM EDTA (pH 8.0)) and was used as the DNA sample. The concentrations of DNA were determined by measurement of the absorbance at 260 nm with a Shimadzu UV-1200 spectrophotometer (Shimadzu, Kyoto, Japan).

Part of the luciferase region in the pDNA pGL3 was amplified by PCR (TaKaRa PCR Thermal Cycler (MP TP3000, TAKARA Bio, Shiga, Japan)) with the primers RHY008 (5′-GTACACGTTCGTCACATCTC-3′) and RHY010(5′-CCTGATACCTGGCAGATGGA-3′) (Proligo Japan, Kyoto, Japan). The reaction mixture (100 μl) consisted of an adequate amount of template, 100 pmols of primers, 1.6 mM dNTP, 2.5 units of Taq DNA polymerase (Ex Taq), 1.5 mM $MgCl_2$, 50 mM KCl and Tris buffer (pH 8.3) (TaKaRa Bio, Shiga, Japan). The PCR was performed by denaturation at 94 °C for 3 min, followed by 30 cycles at 94 °C for 1 min, annealing at 55 °C for 1 min, and extension at 72 °C for 2 min. After the PCR procedure, a 10 μl aliquot of the reaction mixture was subjected to agarose gel (1%) electrophoresis, and the amplified pDNA was quantified by measuring the fluorescence intensity of ethidium bromide bound to the DNA with an ATTO imaging analyzer (AE-6911) (Tokyo, Japan).

Measurement of TFL-3 Associated with Hepatocytes At various time points post-lipofection, cells were washed twice with 3 ml of cold phosphate-buffered saline (PBS, pH 7.4) and harvested by the addition of 1 ml of 0.25% trypsin solution, followed by incubation at 37 °C for 5 min. The cells were then collected by centrifugation (1000 rpm, 5 min, and 4 °C). The collected cells were lysed by incubation with 2 ml CCLR at room temperature for 2 h. An aliquot was used for the measurement of rhodamine intensity using a fluorescent spectrophotometer, F-4500 (Hitachi, Tokyo, Japan). The protein content of the sample was determined with the DC protein assay kit. The data are expressed as the amount of liposome (pmol) per μg of protein.

Statistics All values are expressed as the mean±S.D. Statistical analyses were performed using the GraphPad In-Stat software program (GraphPad Software, CA, U.S.A.). The level of significance was set at $p<0.05$.

RESULTS

Effect of Culture Time Prior to Lipofection on Gene Expression in Primary Cultured Mouse Hepatocytes Mouse hepatocytes were lipofected for 4 h at either 18 or 42 h after a 4 h-preculture. Luciferase activity was determined after 24, 48 or 72 h (Fig. 1). Gene expression was gradually increased in a post-lipofection culture time-dependent manner. In addition, the gene expression in cells that had been cultured for a longer period (42 h) before lipofection was much higher, in total, than in cells cultured for shorter periods (18 h) before lipofection. Interestingly, gene expression mediated by TFL-3 was much higher (approximately 15 fold) than those mediated by LipofectAMINE. This indicates that TFL-3 is superior to LipofectAMINE in terms of lipofection in primary mouse hepatocytes.

Measurement of pDNA Delivered in and TFL-3 Associated with the Hepatocytes Following a 4 h lipofection by TFL-3, the amount of pDNA transported into the hepatocytes was quantitatively determined at either 6 h or 48 h post-lipofection (Fig. 2A). The successful delivery of pDNA to mouse as well as rat hepatocytes occurred at an earlier time point (6 h after lipofection). No significant difference in amounts was found between mouse and rat hepatocytes. The amount dramatically decreased for a longer time point (48 h after lipofection). It appears that the culture time prior to lipofection has an effect on the retention of transported pDNA (Fig. 2A, insertion), although this difference would not reflect gene expression, since the restored pDNA was less than 1% of pDNA delivered at earlier time points.

Under the same experimental conditions, the amount of TFL-3 associated with hepatocytes was also examined (Fig. 2B). There was no significant difference at any of the time points after lipofection. It thus appears that the culture time prior to lipofection has no effect on the amount of TFL-3 bound to the hepatocytes. The amount of bound liposome decreased slightly with increasing time of post-lipofection.

Effect of the Density of Hepatocytes on Lipofection Efficiency A greater gene expression was detected with larger numbers of hepatocytes (Fig. 3). The gene expression for the

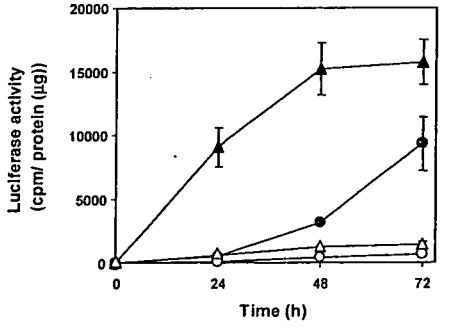

Fig. 1. Effect of Culture Time Prior to Lipofection on Gene Expression in Primary Cultured Mouse Hepatocytes

Isolated mouse hepatocytes (1.5×10^6 cells) were plated in a collagen type-I coated dish (60 mm) and incubated for 4 h (preculture). At 18 h (●, ○) or 42 h (▲, △) after preculture, the cells were lipofected with either pDNA/TFL-3 complexes (closed symbols) or pDNA/LIPOFECTAMINE complexes (open symbols) for 4 h. After removal of the lipoplexes, the cells were further incubated for periods up to 72 h. During incubation at the indicated time points, the luciferase activity (cpm/μg of total protein) in hepatocytes was determined as described in the Materials and Methods. The data represent the mean±S.D.

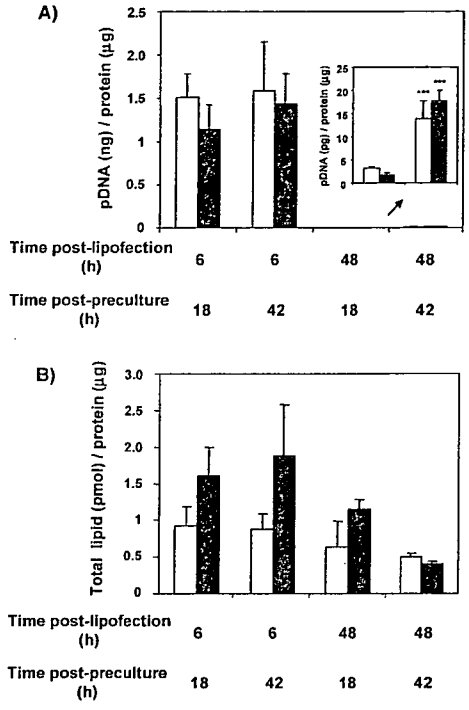

Fig. 2. Amount of pDNA Delivered in and TFL-3 Associated with the Hepatocytes

Isolated mouse (□) and rat (■) hepatocytes (1.5×10^6 cells) were plated and incubated for 4 h (preculture). At 18 h or 42 h after preculture, the cells were lipofected for 4 h. At 6 h or 48 h post-lipofection, the amounts of pDNA in the cells (A) and TFL-3 bound to the cells (B) were determined as described in the Materials and Methods. The data represent the mean±S.D.

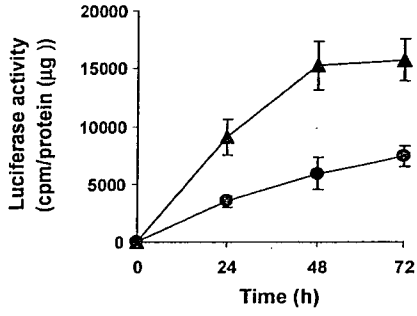

Fig. 3. Effect of Density of Hepatocytes on Lipofection Efficiency

Isolated mouse hepatocytes (0.75×10^6 (●) or 1.5×10^6 (▲) cells) were plated in a collagen type-I coated dish (60 mm) and incubated for 4 h (preculture). At 42 h after preculture, the cells were lipofected for 4 h. At 6 h or 48 h post-lipofection, the amounts of pDNA in the cells and TFL-3 bound to the cells were determined as described in the Materials and Methods. The data represent the mean±S.D. After removal of the lipoplexes, the cells were further incubated up to 72 h. During incubation at the indicated time points, luciferase activity (cpm/μg of total protein) in hepatocytes was determined, as described in the Materials and Methods. The data represent the mean±S.D.

case of higher cell density was relatively 2—3 folds larger that those for the case of a lower cell density. At a higher cell density, gene expression increased, reaching a maximum level up to 48 h. To the contrary, at a lower cell density, gene expression still gradually increased in a culture time postlipofection-dependent manner.

In addition, the viability of hepatocytes was monitored throughout this study. Viability gradually decreased in a culture time-dependent manner with or without lipofection (data not shown), although the efficiency of gene expression relatively increased.

DISCUSSION

Among the currently available therapeutic options, hepatocyte transplantation is a promising procedure. Therefore, a combination of hepatocyte transplantation and *in vitro* hepatocyte-targeted gene transfer represents an important strategy for expanding the treatment options for liver disease. TFL-3 may be a candidate for *in vitro* gene transfer targeted to hepatocytes, since we recently reported that TFL-3[4] achieved sufficient gene expression in primary cultured rat hepatocytes.[5] However, a widely applied approach to support cross-species is needed with TFL-3 before human applications. Therefore, in this study, we further examined the utility of TFL-3 on transgene expression in another rodent hepatocyte. If some differences on the gene expression between mouse hepatocytes and rat ones were obtained although both animals are rodent. This would suggest that there is a species difference on the gene expression by hepatocytes.

As a first matter, the issue of whether TFL-3 can be successfully used to achieve gene expression in primary cultured mouse hepatocytes was examined. As shown in Fig. 1, efficient gene expressions could be achieved using TFL-3 and the level of gene expression was dependent on the culture time prior to lipofection. In addition, the transgene activity was superior to that of the commercially available LipofectAMINE under our experimental conditions, which is consistent with the result showing the LipofectAMINE does not work very well in the presence of serum.[12] These observations are consistent with the result obtained with rat hepatocytes.[4] These findings suggest that TFL-3 could be useful vector for achieving a sufficient level of gene expression in rodent hepatocytes.

Interestingly, gene expression in mouse hepatocytes was relatively much higher (2—2.5 fold) than those in the rat hepatocytes. In addition, the peak for maximum gene expression level in mouse hepatocytes appeared to move to a later time point post-lipofection, compared to the results reported for rat hepatocytes.[5] This is supported by the report of Weglarz *et al.*[13,14] demonstrating that the peak for DNA replication after a partial hepatectomy in rats, presumably in hepatocytes, occurs at 24 h after the operation while it takes place at 44 h in mice. It appears that the difference in DNA replication is due to the difference in the length of G1 between rat and mouse hepatocytes.[15] This suggests that there may be a species difference in exogenous gene expression by the hepatocytes as a result of transfection with TFL-3.

The time of culture prior to lipofection had no effect on the amount of pDNA delivered to rodent hepatocytes (Fig. 2A), while gene expression was obviously dependent on the time of culture prior to lipofection (Fig. 2).[5] Similar results have also been reported for other mammalian line cells.[16] These findings suggest that gene expression is not necessarily related to the amount of pDNA delivered by TFL-3, but rather to the biological condition of the hepatocytes that influences, for example, the process of transcription of the delivered pDNA. Of course, the delivery of a sufficient amount of pDNA to the cell and nucleus to permit gene expression is an absolute requisite.

As described in Fig. 3, gene expression increased with increasing cell density. This observation is inconsistent with our earlier results for rat hepatocytes[5] and other's.[17] This

discrepancy may be due to differences in experimental conditions; 0.75×10^6 and 1.5×10^6 cells for the mouse study and 1.5×10^6 or 3×10^6 cells for the rat study.[5] Gene expression in rat hepatocytes might have already reached the maximum level at a lower cell density (1.5×10^6). Hence, the resulting gene expression may decrease at higher cell density (3.0×10^6). Although the reason for why efficient gene expression was achieved for a lower cell density of hepatocytes is currently unclear, the increased cellular interaction at higher cell density might induce some signal transduction, which would inhibit protein production in the cells. Further study will be required to confirm this assumption.

The results presented here indicate that the conditions used for lipofection are critical for achieving an efficient gene expression in primary cultured hepatocytes. This strongly indicates that an increased gene expression in rodent hepatocytes could be achieved by optimizing the lipofection conditions, such as the time of culture prior to lipofection, the time used for lipofection and the density of the cells. In addition, the results described here and earlier[5] demonstrate that the TFL-3 may be a suitable non-viral vector system for successful gene expression in non- or less-dividing cells. Therefore, for developing further efficient delivery system with TFL-3 for clinical use, it will be important to collect more information on the biological conditions that affect the transcription process of target cells.

Acknowledgments We thank Dr. Hiroshi Kikuchi, Daiichi Pharmaceutical, for helpful suggestions and Dr. Milton S. Feather for his helpful advice in writing the English manuscript.

REFERENCES

1) Zhang G., Budker V., Wolff J. A., *Hum. Gene Ther.*, **10**, 1735—1737 (1999).
2) Liu F., Song Y., Liu D., *Gene Ther.*, **6**, 1258—1266 (1999).
3) Rossmanith W., Chabicovsky M., Herkner K., Schulte-Hermann R., *DNA Cell Biol.*, **21**, 847—853 (2002).
4) Kikuchi A., Aoki Y., Sugaya Y., Serikawa T., Takakuwa K., Tanaka K., Suzuki N., Kikuchi H., *Hum. Gene Ther.*, **10**, 947—955 (1999).
5) Nguyen L. T., Ishida T., Ukitsu S., Li W. H., Tachibana R., Kiwada H., *Biol. Pharm. Bull.*, **26**, 880—885 (2003).
6) Demetriou A. A., Felcher A., Moscioni A. D., *Dig. Dis. Sci.*, **36**, 1320—1326 (1991).
7) Rhim J. A., Sandgren E. P., Degen J. L., Palmiter R. D., Brinster R. L., *Science*, **263**, 1149—1152 (1994).
8) Wang X., Zhao X., Andersson R., *Eur. J. Surg.*, **161**, 475—481 (1995).
9) Vogels B. A., Maas M. A., Bosma A., Chamuleau R. A., *Cell Transplant.*, **5**, 369—378 (1996).
10) Tanaka K., Sato M., Tomita Y., Ichihara A., *J. Biochem.* (Tokyo), **84**, 937—946 (1978).
11) Serikawa T., Suzuki N., Kikuchi H., Tanaka K., Kitagawa T., *Biochim. Biophys. Acta*, **1467**, 419—430 (2000).
12) Tachibana R., Harashima H., Shinohara Y., Kiwada H., *Adv. Drug Deliv. Rev.*, **52**, 219—226 (2001).
13) Weglarz T. C., Degen J. L., Sandgren E. P., *Am. J. Pathol.*, **157**, 1963—1974 (2000).
14) Weglarz T. C., Sandgren E. P., *Proc. Natl. Acad. Sci. U.S.A.*, **97**, 12595—12600 (2000).
15) Fausto N., Campbell J. S., *Mech. Dev.*, **120**, 117—130 (2003).
16) Li W., Ishida T., Tachibana R., Almofti M. R., Wang X., Kiwada H., *Int. J. Pharm.*, **276**, 67—74 (2004).
17) Watanabe Y., Nomoto H., Takezawa R., Miyoshi N., Akaike T., *J. Biochem.* (Tokyo), **116**, 1220—1226 (1994).

THE JOURNAL OF GENE MEDICINE
J Gene Med 2006; 8: 324–334.
Published online 16 November 2005 in Wiley InterScience (www.interscience.wiley.com). DOI: 10.1002/jgm.850

RESEARCH ARTICLE

Stimulatory effect of polyethylene glycol (PEG) on gene expression in mouse liver following hydrodynamics-based transfection

Tatsuhiro Ishida
Wenhao Li
Zhihui Liu
Hiroshi Kiwada*

Department of Pharmacokinetics and Biopharmaceutics, Faculty of Pharmaceutical Sciences, The University of Tokushima, 1-78-1 Sho-machi, Tokushima 770-8505, Japan

*Correspondence to:
Hiroshi Kiwada, Department of Pharmacokinetics and Biopharmaceutics, Faculty of Pharmaceutical Sciences, The University of Tokushima, 1-78-1 Sho-machi, Tokushima 770-8505, Japan.
E-mail:
hkiwada@ph.tokushima-u.ac.jp

Received: 10 February 2005
Revised: 26 August 2005
Accepted: 7 September 2005

Abstract

Background Rapid intravenous injection of a large volume of plasmid DNA (pDNA), i.e. a transfection procedure based on hydrodynamics, is known to be an efficient and liver-specific method of *in vivo* gene delivery. However, the gene expression is transient.

Methods We investigated the effect of addition of polyethylene glycol (PEG) to a solution of naked pDNA (luciferase) on the expression of the gene in mouse liver following transfection by the hydrodynamics-based technique. In addition, the mechanism leading to the enhancement of the gene expression was studied.

Results The addition of 1% (w/v) PEG2000 to the pDNA solution enhanced the resulting gene expression in the liver. Increasing the PEG2000 concentration to more than 1 and up to 10% (w/v) rather diminished the gene expression level. By contrast, increasing the molecular weight of PEG to over 2000 up to 10000 did not affect the level of gene expression. Histopathological and serum-chemistry examinations indicated that hydrostatic or osmotic pressure increased tissue and hepatocellular damage in a PEG-concentration-dependent manner, and resulted in a decrease in gene expression. Quantitative evaluation showed that the enhanced gene expression resulted from stabilization of the pDNA introduced into the hepatocytes and an enhancement of the transport of *intact* pDNA to the nucleus.

Conclusions For most gene therapy applications and gene function studies, sustained expression of the introduced gene(s) is necessary. This simple method to achieve enhanced gene expression in liver may have a great potential for a wide variety of laboratory studies in molecular and cellular biology as well as possibly for future clinical applications in humans.

Keywords polyethylene glycol (PEG); hydrodynamics-based transfection; gene delivery; liver; hepatocytes; naked DNA

Introduction

The transfection of plasmid DNA (pDNA) into living animals is an indispensable tool in molecular and cellular biology. The avalanche of new genes discovered as part of the human genome project has further increased the importance of gene transfer in understanding gene function. However,

the analysis of gene expression in living animals has been limited since it has required complicated laboratory procedures such as the implantation of transfected cells or generation of transgenic animals. There is an obvious need for simple methods that allow for efficient gene transfer into cells to achieve high transgene expression *in vivo* for gene function studies.

One of the alternatives is the direct use of naked pDNA. Since the initial report in the early 1990s of the successful expression of a reporter gene in muscle by simple intramuscular injection of pDNA [1], there have been many *in vivo* studies demonstrating successful transgene expression in liver [2–5], lung [6], heart [7], and skin [8]. The single use of naked pDNA has the advantage that it does not require the laborious procedures for preparation and purification connected with the use of viral vectors; it lacks the immunogenecity and oncogenic effects of viral vector systems, and the hazard of endogenous virus recombination [9,10]. On the other hand, the use of naked pDNA has a severe limitation in that it requires local or regional administration or surgical procedures. In addition, the level of transgene expression resulting from such local injection is relatively low and restricted to the injection site.

Another adapted alternative, the hydrodynamics-based procedure, has been reported by Liu *et al.* [11] and Zhang *et al.* [5]. By rapid injection of pDNA in a large volume into a mouse tail vein they achieved high levels of foreign gene expression in mouse liver, particularly in hepatocytes. Under these conditions, a high hydrostatic pressure is generated in the inferior vena cava and in the vein linked to that vessel because the volume and speed of injection exceed the cardiac output. The mechanism of gene transfer by this procedure is not clearly understood but must be related to an enhanced uptake and intracellular processing of the injected pDNA in the hepatocytes. To date, the hydrodynamics-based transfection procedure has been utilized by the gene therapy community for the evaluation of therapeutic activities of various genes (see, for reviews, Liu and Knapp [12] and Horweijer and Wolff [13]). Other reported applications of this technique include studies to define the regulatory functions of DNA sequences [14–16], investigations to evaluate gene suppression activity of siRNA [17–20], and experiments to establish animal models for viral infection [21]. Despite many desirable features of the hydrodynamics-based procedure such as simplicity, convenience, and high efficiency, further improvements to this procedure are required because the transgene expression is transient.

Polyethylene glycol (PEG) is a hygroscopic, water-soluble, and relatively chemically inert synthetic polymer [22] having a variety of effects on biological systems [23–26]. In earlier days, PEG was used as a cell-cell fusogen for the production of somatic hybrids [27]. Dehydration of lipid membranes by PEG has been suggested to be critical for the ability of this polymer to induce membrane fusion [28,29]. Osmotic effects are also considered to be of importance. An osmotic imbalance due to the osmolyte gradient between the exclusion layer and the bulk PEG solution is assumed to result in stress that is considered to lead to an increase in membrane permeability [30].

Most recently, Zhang *et al.* [31] proposed that the hydrodynamic injection induces a transient irregularity of the heart function, a sharp increase in venous pressure, an enlargement of liver fenestrae, and enhancement of membrane permeability of the hepatocytes. This report led us to hypothesize that PEG, if added to a large volume of pDNA solution, might increase the membrane permeability of the hepatocytes and consequently allow large amounts of pDNA into the hepatocytes, resulting in enhanced transgene expression in the liver compared to the regular hydrodynamics-based procedure. In this study we examined this hypothesis and we show that it is correct.

Materials and methods

Materials and animals

Plasmid pGL3-Control (pDNA) containing the cDNA of firefly luciferase driven by the SV40 promoter, the luciferase assay kit and cell culture lysis reagent (CCLR) were purchased from Promega (WI, USA). PEGs with average molecular weights of 2000, 6000 and 10 000 were from Boehringer Mannheim (Mannheim, Germany). Evans Blue was purchased from Nacalai Tesque (Kyoto, Japan). Collagenase type I and bromo-2′-deoxyuridine (BrdUrd) were purchased from Sigma (MO, USA). RPMI1640 medium was purchased from Nissui Pharmaceutical (Tokyo, Japan). Antibiotics (penicillin and streptmicin) were purchased from ICN Biomedical (OH, USA). All other reagents were of analytical grade.

Mice and hydrodynamic injection

ddY male mice, 4 weeks old, 18–20 g, were purchased from Japan SLC (Shizuoka, Japan). All animal experiments were evaluated and approved by the Animal and Ethics Review Committee of the Faculty of Pharmaceutical Sciences, The University of Tokushima. Animals were injected via the tail vein with a large volume of saline (2 ml) containing 40 μg of pDNA in 5 s according to a previously published procedure [11]. Saline was used as a carrier solution for injection. The indicated concentrations of PEG with the estimated average molecular weights were added to the carrier solution.

Luciferase assay

Luciferase activity in the tissue was determined according to an established procedure [11,32] with minor modifications. Briefly, approximately 200 mg of liver tissue were homogenized in 1 ml of the CCLR and then frozen and thawed three times, followed by centrifugation for

10 min at 4 °C and 20 000 *g*. The supernatant was diluted, if needed, using the CCLR. A 10-µl aliquot of the diluted sample was used to determine the luciferase activity using luciferase assay reagent according to the manufacturer's recommended protocol (Promega, WI, USA). The protein content of the sample was measured with the DC protein assay kit (Bio-Rad Laboratories, CA, USA), and the data are expressed as light counts/s/mg of protein.

Serum-chemistry assay

Mice were injected using the hydrodynamics-based procedure (2 ml/mouse/5 s) in the presence of either 0, 1 or 10% (w/v) PEG2000. Blood was collected by heart puncture by using a heparinized syringe under ether anesthesia at 3 h, 12 h, 24 h and 7 days after the injection. Blood samples were collected in a tube containing an SST gel and a clot activator (Eiken, Tokyo, Japan), allowed to stand for 30 min at room temperature, and then centrifuged at 3000 rpm for 15 min to collect serum. Sera were stored at −80 °C until use. A Hitachi 7170 automatic analyzer (Tokyo, Japan) was used to measure aspartate aminotransferase (AST) and alanine aminotransferase (ALT).

Vascular permeability assay

In order to quantify blood vessel permeability in the liver after hydrodynamic injection, Evans Blue dye solution (0.2 mg in 2 ml of saline) containing 0, 1 or 10% (w/v) PEG2000 was injected into the tail vein with the hydrodynamics-based procedure. For the same purpose, the dye (0.2 mg in 0.2 ml of saline) was injected either 5 or 30 min after the hydrodynamic injection of saline containing 0, 1 or 10% (w/v) PEG2000 had been administered. At 6 h after the first injection, the liver was removed, and the dye was extracted. The ground liver tissue (200 mg) was dissolved in 1 ml of tissue solubilizer (2 N KOH in isopropanol) at 60 °C overnight. The solution was allowed to cool before the addition of 2 ml of ethyl acetate; the mixture was then vortexed, and 2 ml of 1 N HCl were added, vortexed again, and centrifuged at 2000 *g* for 15 min. Absorption of the upper phase at 626 nm was recorded. Concentrations were determined from a standard curve of Evans Blue dye.

Histological evaluation

To evaluate tissue and cellular damage in the liver following hydrodynamic injection, mice were injected with saline or saline containing the indicated concentrations of PEG2000. At 10 min after injection, the mice were sacrificed and livers were collected. The livers were separated and the separate lobes were fixed in 20% neutral-buffered formalin. After embedding in paraffin, the lobes were sectioned in slices of 5 µm thickness. The paraffin sections were used for histopathological analysis (hematoxylin and eosin staining). The histopathological scores were recorded under microscope observation.

Isolation of hepatocytes

Hepatocytes were isolated from the livers by the *in situ* perfusion method established previously [33]. Briefly, mice were anesthetized with sodium pentobarbital and the portal vein was cannulated. Hanks' balanced salt solution containing 0.5 mM EGTA and 10 mM HEPES was perfused at approximately 40 ml/min for 4 min. Then, 0.0125% collagenase type I in RPMI1640 medium containing antibiotics (100 units/ml penicillin and 100 µg/ml streptmicin), prepared just prior to use, was perfused at 20 ml/min for 6 min. Following these perfusions, the liver was carefully removed and dissected, and the cells were dispersed in cold Hanks' solution and the suspension was filtered over a cell strainer (Becton Dickinson Labware, NJ, USA) with a 100-µm mesh to obtain a single-cell suspension. Parenchymal cells (hepatocytes) were separated from non-parenchymal cells by differential centrifugation at 50 *g* for 90 s. The precipitate (hepatocytes) was resuspended in RPMI1640 medium containing antibiotics supplemented with 5% heat-inactivated fetal bovine serum (Sigma, MO, USA). In each preparation, the viability of the isolated cells was determined by trypan blue exclusion.

Isolation of nuclei of hepatocytes

The isolated hepatocytes (1×10^6 cells) were suspended in 0.5 ml of lysis buffer (0.5% Nonidet P-40, 10 mM Tris, 10 mM NaCl, 3 mM $MgCl_2$, pH 7.4) to destabilize the plasma membrane. The nuclear fraction in the suspension was collected as a precipitate by centrifugation (1400 *g*, 5 min, 4 °C). To prevent the detection of extranuclear pDNAs, the nuclear fraction was treated with *Hind*III (Nippon Gene, Tokyo, Japan), for which a recognition site exists in the amplified region of pGL3 (37 °C, 1 h). The treated solution was centrifuged again. The precipitate was used as the nuclear fraction.

Quantitative determination of pDNA delivered in the hepatocytes

The pDNA delivered to hepatocytes was quantitatively determined using a method recently developed in our laboratory [34] with minor modifications. Briefly, the isolated hepatocytes (1×10^6 cells) were suspended in 0.5 ml of lysis buffer (0.5% Nonidet P-40, 10 mM Tris, 10 mM NaCl, 3 mM $MgCl_2$, pH 7.4) to destabilize the plasma membrane. Aliquots of the suspension were subjected to polymerase chain reaction (PCR) study. Part of the luciferase region in the pGL3 pDNA was amplified by PCR using a thermal cycler (MP TP3000; TaKaRa Bio, Shiga, Japan) with primers RHY008

(5′-GTACACGTTCGTCACATCTC-3′) and RHY010 (5′-CCTGATACCTGGCAGATGGA-3′) (Proligo Japan, Kyoto, Japan). The reaction mixture (100 μl) consisted of an adequate amount of template, 100 pmol of the primers, 1.6 mM dNTP, 2.5 units of Taq DNA polymerase (Ex Taq), 1.5 mM $MgCl_2$, 50 mM KCl and Tris buffer (pH 8.3) (TaKaRa Bio). The PCR was performed by denaturation at 94 °C for 3 min, followed by 30 cycles at 94 °C for 1 min, annealing at 55 °C for 1 min, and extension at 72 °C for 2 min. After the PCR procedure, 10 μl of the reaction mixture were subjected to agarose gel (1%) electrophoresis, and the amplified pDNA was quantified by measuring the fluorescence intensity of ethidium bromide bound to the DNA with an ATTO imaging analyzer (AE-6911, Tokyo, Japan).

Quantitative determination of pDNA delivered in the nuclei of hepatocytes

To extract nuclear DNA (containing pDNA), the nuclear fraction prepared as described above was resuspended in 0.5 ml of Tris-HCl buffer (10 mM Tris, 10 mM NaCl, 3 mM $MgCl_2$, pH 7.4) containing 10 mM EDTA and 0.1% sodium dodecyl sulfate (SDS), and proteinase K (Merck, Frankfurt, Germany) was added at a final concentration of 0.1 mg/ml. After incubation at 37 °C overnight, proteins were eliminated by phenol/chloroform treatment and the DNA was precipitated by the addition of ethanol. The precipitate was dissolved in TE buffer (10 mM Tris-HCl, 1 mM EDTA; pH 8.0) and used as a pDNA sample. Concentrations of DNA were determined by measurement of the absorbance at 260 nm with a Shimadzu UV-1200 spectrophotometer (Kyoto, Japan).

For quantitative analysis, the prepared DNA sample was divided into two portions to determine the amount of pDNA delivered in nuclei and the amount of intact pDNA in the nuclei that kept the luciferase-coding region in the sequence intact.

The amount of pDNA delivered in the nuclei

Part of the luciferase region in the pGL3 pDNA was amplified by PCR (TaKaRa PCR thermal cycler, MP TP3000; TaKaRa Bio) with primers RHY008 (5′-GTACACGTTCGTCACATCTC-3′) and RHY010 (5′-CCTGATACCTGGCAGATGGA-3′) (Proligo Japan). The reaction mixture (100 μl) consisted of an adequate amount of template, 100 pmol of the primers, 1.6 mM dNTP, 2.5 units of Taq DNA polymerase (Ex Taq), 1.5 mM $MgCl_2$, 50 mM KCl and Tris buffer (pH 8.3) (TaKaRa Bio). The PCR was performed by denaturation at 94 °C for 3 min, followed by 30 cycles at 94 °C for 1 min, annealing at 55 °C for 1 min, and extension at 72 °C for 2 min. After the PCR procedure, 10 μl of the reaction mixture were subjected to agarose gel (1%) electrophoresis, and the amplified pDNA was quantified by measuring the fluorescence intensity of ethidium bromide bound to the DNA with an ATTO imaging analyzer (AE-6911).

The amount of intact pDNA in the nuclei

Aliquots of pDNA sample were subjected to agarose gel (1%) electrophoresis. After electrophoresis, the gel was stained for 15 min at room temperature in ethidium bromide solution (0.5 mg/ml). The bands of pDNA were visualized by ultraviolet irradiation and the region of the gel containing intact pDNA (non-degradated) was excised. The intact pDNA was purified from the agarose with a GENECLEAN kit (BIO101, CA, USA). The recovered intact pDNA was subjected to PCR, and the amplified pDNA was quantified, as described above.

Statistics

All values were expressed as the mean ± standard deviation (S.D.). Statistical analyses were performed using GraphPad InStat software (GraphPad Software, CA, USA). The level of significance was set at $p < 0.05$.

Results

Effect of PEG concentration on gene expression in the liver

Luciferase activity in tissues was determined at 12 and 24 h after the hydrodynamic injection of 40 μg pDNA containing 1, 2, 5 or 10% (w/v) PEG2000. Injection without PEG (regular hydrodynamic injection) served as a control. In all our experiments low luciferase activity was detected in lung, spleen and kidney (data not shown); extensive gene expression was detected in only liver. At 12 h after injection, the expressed luciferase activities in the liver were lower in the PEG-containing groups than in the control livers (Figure 1). In addition, the expression levels decreased with increasing PEG concentration (Figure 1). Surprisingly, with prolonged time after injection, luciferase activity was enhanced, irrespective of the PEG concentration. By contrast, the luciferase level induced by the regular hydrodynamic injection rather declined as time proceeded. It is worthwhile to note that the highest concentration of PEG (10% (w/v)) diminished the expressed luciferase level induced by regular hydrodynamic injection. It seems that there is an optimal concentration of PEG to cause enhancement of gene expression. On the basis of the result described in Figure 1, 1% (w/v) PEG2000 was adopted for all subsequent experiments.

We also examined the effect of PEG on gene expression induced by conventional injection (40 μg pDNA in 200 μl of saline). At 12 and 24 h after the injection, the gene expression levels were much lower than those induced by the hydrodynamic injection, and no enhancing effect of PEG on the gene expression was observed (data not shown).

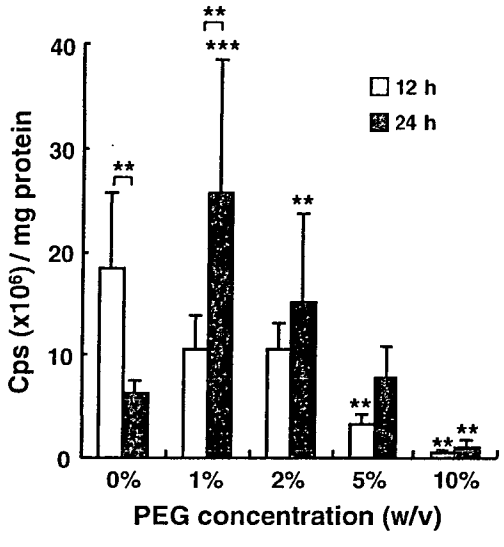

Figure 1. Effect of PEG concentration on gene expression in the liver. Mice were injected with a large volume of pDNA solution (40 μg pDNA) containing 0, 1, 2, 5 or 10% (w/v) PEG2000 using the hydrodynamics-based procedure (2 ml/mouse/5 s). Luciferase activity in the liver was determined at 12 and 24 h after injection. Data are presented as mean ± S.D. (n = 3). Statistical significance against 0% PEG2000 (regular hydrodynamic injection) was analyzed by Student's *t*-test. Statistical significance between gene expressions levels at different time points (12 and 24 h) after hydrodynamics-based transfection was also analyzed by Student's *t*-test. $^{**}p < 0.01$; $^{***}p < 0.005$

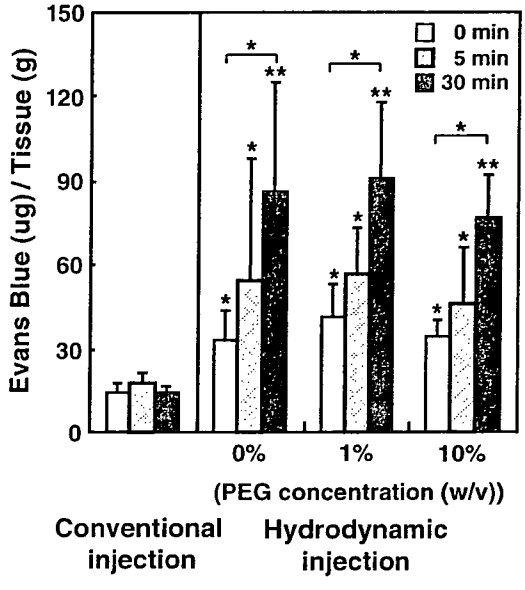

Figure 2. Effect of PEG on vascular permeability and/or hepatocyte-membrane permeability. Evans Blue dye (0.2 mg in 2 ml of saline) containing 0, 1 or 10% (w/v) PEG2000 was injected into the tail vein with the hydrodynamics-based procedure. The dye (0.2 mg in 0.2 ml of saline) was injected at either 5 or 30 min after the hydrodynamic injection of saline containing 0, 1 or 10% (w/v) PEG2000. At 6 h after the first injection, the liver was removed, the dye was extracted and quantified. Data are the mean ± S.D. (n = 3). Statistical significance against conventional injection was analyzed by Student's *t*-test. Statistical significance between gene expression levels at different time points after hydrodynamics-based transfection was analyzed by one-way ANOVA. $^{*}p < 0.05$; $^{**}p < 0.01$

Effect of PEG chain length on gene expression in the liver

PEG chain length may affect the permeability-enhancing effect of PEG on hepatocyte membranes, possibly resulting in a further enhancement of gene expression in the liver. To test this, we added 1% (w/v) of PEG6000 or PEG10000 instead of PEG2000 to the pDNA solution and injected it hydrodynamically into mice. The livers showed no significant increase in luciferase levels at 12 or 24 h after injection, compared to the values obtained with 1% (w/v) PEG2000 (data not shown). On the basis of this result and those described in Figure 1, we adopted 1% (w/v) PEG2000 to add to the pDNA solution for all subsequent experiments.

Effect of PEG on vascular permeability and/or hepatocyte membrane permeability

To examine the effect of PEG on the vascular permeability and/or hepatocyte membrane permeability, the mice were treated with the hydrodynamic injection or a conventional injection. Subsequently, they were treated with a conventional injection of Evans Blue solution (200 μl), which is one of the most commonly used markers for membrane permeability [35]. The hydrodynamic injection resulted in a significant increase in the level of Evans Blue in the liver, compared to the conventional injection (Figure 2). This effect was observed regardless of the PEG concentration and time after hydrodynamic injection. Interestingly, the concentration of Evans Blue in the liver increased with increasing the time interval between the two injections.

Liver damage following rapid injection with a large volume of PEG-containing pDNA solution

To examine whether PEG might cause more severe liver damage relative to the regular hydrodynamics-based procedure, liver histology was examined by histopathological evaluation. Figure 3 shows liver sections of mice receiving a small volume of pDNA solution (a conventional injection) or a large volume of pDNA solution with or without PEG2000 (1 or 10% (w/v)) within 5 s (the hydrodynamic injection).

While no histological abnormalities were observed in the liver following the normal injection (Figure 3A), injection via the hydrodynamics-based procedure caused significant liver damage regardless of the presence or absence of PEG (Figures 3B, 3C, and 3D). Following the hydrodynamic injection, hepatocytes showed degeneration with